Wavelets on the Interval and Fast Wavelet Transforms

Albert Cohen, Ingrid Daubechies, Pierre Vial

Wavelets on the Interval and Fast Wavelet Transforms

ALBERT COHEN

CEREMADE, Université Paris–Dauphine, 75775 Paris Cedex 16, France

INGRID DAUBECHIES

Mathematics Department, Rutgers University, New Brunswick, New Jersey 08903, and AT&T Bell Laboratories, Murray Hill, New Jersey 07974

AND

PIERRE VIAL

Faculté des Sciences, St. Jérome, Université de Marseille, 13397 Marseille Cedex 13, France

We discuss several constructions of orthonormal wavelet bases on the interval, and we introduce a new construction that avoids some of the disadvantages of earlier constructions.

1. INTRODUCTION

The construction of orthonormal wavelet bases or of pairs of dual, biorthogonal wavelet bases for $L^2(\mathbb{R})$ is now well understood. For the construction of orthonormal bases of compactly supported wavelets for $L^2(\mathbb{R})$, in particular, one starts with a trigonometric polynomial

$$m_0(\xi) = \sum_n c_n e^{-in\xi} \tag{1.1}$$

satisfying

$$m_0(0) = 1 \tag{1.2}$$

and

$$|m_0(\xi)|^2 + |m_0(\xi + \pi)|^2 = 1, \tag{1.3}$$

as well as some mild technical conditions. (Necessary and sufficient conditions are given by Cohen [7] and Lawton [17, 18]. A sufficient but not necessary condition, always satisfied in practice, is $|m_0(\xi)| \neq 0$ for all $|\xi| \leq \pi/2$; see Mallat [19]. One then defines the corresponding scaling function ϕ and wavelet ψ by

$$\hat{\phi}(\xi) = (2\pi)^{-1/2} \prod_{j=1}^{\infty} m_0(2^{-j}\xi) \tag{1.4}$$

$$\hat{\psi}(\xi) = e^{-i\xi/2} \overline{m_0(\xi/2 + \pi)} \hat{\phi}(\xi/2), \tag{1.5}$$

where $\wedge$ denotes the Fourier transform, normalized by $\hat{f}(\xi) = (2\pi)^{-1/2} \int dx e^{-i\xi x} f(x)$. The functions $\psi_{j,k}(x) = 2^{-j/2} \times \psi(2^{-j}x - k)$, $j, k \in \mathbb{Z}$, then constitute an orthonormal basis for $L^2(\mathbb{R})$. For fixed $j \in \mathbb{Z}$, the $\phi_{j,k}(x) = 2^{-j/2}\phi(2^{-j}x - k)$ are an orthonormal basis for a subspace $V_j \subset L^2(\mathbb{R})$; the spaces V_j constitute a multiresolution analysis, meaning in particular that

$$\cdots \subset V_2 \subset V_1 \subset V_0 \subset V_{-1} \subset V_{-2} \subset \cdots,$$

with

$$\bigcap_{j \in \mathbb{Z}} V_j = \{0\}, \quad \overline{\bigcup_{j \in \mathbb{Z}} V_j} = L^2(\mathbb{R})$$

and

$$\mathrm{Proj}_{V_{j-1}} f = \mathrm{Proj}_{V_j} f + \sum_{k \in \mathbb{Z}} \langle f, \psi_{j,k} \rangle \psi_{j,k}.$$

(See Mallat [19], Meyer [20], or Daubechies [9, 10] for more details.)

A consequence of (1.4) is that $\hat{\phi}(\xi) = m_0(\xi/2)\hat{\phi}(\xi/2)$, or

$$\phi(x) = \sqrt{2} \sum_n h_n \phi(2x - n),$$

where the $h_n = \langle \phi, \phi_{-1,n} \rangle$ are proportional to the Fourier coefficients of m_0, $h_n = \sqrt{2} c_n$, where the c_n are as in (1.1).

One can prove (see, e.g., Daubechies [10]) that smoothness for ψ implies that m_0 has to have a zero at π of sufficiently high multiplicity. More precisely,

$$\psi \in C^k(\mathbb{R}) \Rightarrow \int dx\, x^l \psi(x) = 0 \quad l = 0, \ldots, k$$

$$\Updownarrow$$

$$\frac{d^l}{d\xi^l} m_0 \Big|_{\xi=\pi} = 0 \quad l = 0, \ldots, k. \tag{1.6}$$

This in turn implies that m_0 has at least $2k$ non-zero coefficients.

By far the oldest example of such an orthonormal basis of compactly supported wavelets is the Haar basis, with

$$m_0(\xi) = \tfrac{1}{2}(1 + e^{-i\xi})$$

and

$$\phi(x) = \begin{cases} 1 & \text{for } 0 \leq x < 1 \\ 0 & \text{otherwise,} \end{cases}$$

$$\psi(x) = \begin{cases} 1 & \text{for } 0 \leq x < 1/2 \\ -1 & \text{for } 1/2 \leq x < 1 \\ 0 & \text{otherwise.} \end{cases}$$

In this case ϕ and ψ have support widths 1, but they are not continuous, and therefore are unsuitable for the study of continuous function spaces.

Other examples, with more smoothness, were constructed in Daubechies [9]. They correspond to m_0 of the type

$$m_0(\xi) = \left(\frac{1 + e^{-i\xi}}{2} \right)^N Q_N(\xi), \tag{1.7}$$

where $Q_N(\xi)$ is a polynomial of order $N - 1$ in $e^{-i\xi}$, obtained by "spectral factorization" from

$$|Q_N(\xi)|^2 = P_N(\xi) = \sum_{n=0}^{N-1} \binom{N-1+n}{n} \left(\sin^2 \frac{\xi}{2} \right)^n.$$

The resulting ϕ and ψ have support width $2N - 1$, which is the shortest possible under the constraint that m_0 has a zero of order N at $\xi = \pi$. The smoothness of ϕ and ψ in this family of examples increases linearly with N; in particular, there exists $\mu \simeq 0.2$ such that $\phi, \psi \in C^{\mu N}$.

These smoother wavelets provide not only orthonormal bases for $L^2(\mathbb{R})$, but also unconditional bases for function spaces consisting of more regular functions. In particular (Meyer [20]), if $\psi \in C^r(\mathbb{R})$, then the $\phi_{0,k}$, $k \in \mathbb{Z}$, and $\psi_{-j,k}$, $j \in \mathbb{N}$, $k \in \mathbb{Z}$, provide an unconditional basis for the function spaces $C^s(\mathbb{R})$, for all $s < r$. (One needs one "layer" of scaling functions in this case, because constant functions, e.g., are in $C^s(\mathbb{R})$ and cannot be written as combinations of $\psi_{j,k}$. This layer of scaling functions is chosen at the coarsest resolution level under consideration; it need not be the level with label 0.) The reason wavelet bases (unlike Fourier series) can provide unconditional bases for C^r-spaces is essentially that the wavelets ψ have vanishing moments, as guaranteed by (1.6) or (1.7).

There is another way of interpreting the condition (1.6). Since the functions $\phi(\cdot - n)$, $n \in \mathbb{Z}$, are independent, it is equivalent to requiring that any polynomial of degree less than or equal to $N - 1$ can be written as a linear combination of the $\phi(x - n)$ (see Fix and Strang [13] and Cavaretta *et al.* [6]). Since ψ is orthogonal to all the $\phi(\cdot - n)$, this then ensures that the first N moments of ψ, $\int dx\, x^n \psi(x)$ for $n = 0, \ldots, N - 1$, all vanish.

Except for the Haar basis, and unlike many examples with infinite support, the basic wavelet in an orthonormal basis of compactly supported wavelets cannot have a symmetry or antisymmetry axis. Symmetry can be recovered, without giving up the compact support, if the orthogonality requirement is relaxed. In that case one builds two different (but related) multiresolution hierarchies of spaces, $\cdots \subset V_2 \subset V_1 \subset V_0 \subset V_{-1} \subset V_{-2} \subset \cdots$ and $\cdots \subset \tilde{V}_2 \subset \tilde{V}_1 \subset \tilde{V}_0 \subset \tilde{V}_{-1} \subset \tilde{V}_{-2} \subset \cdots$, corresponding to two scaling functions ϕ and $\tilde{\phi}$ and two wavelets ψ and $\tilde{\psi}$. They are defined by means of two trigonometric polynomials m_0 and $\tilde{m}_0$, solutions to

$$m_0(\xi)\overline{\tilde{m}_0(\xi)} + m_0(\xi + \pi)\overline{\tilde{m}_0(\xi + \pi)} = 1; \tag{1.8}$$

instead of (1.4), (1.5) we then have

$$\hat{\phi}(\xi) = (2\pi)^{-1/2} \prod_{j=1}^{\infty} m_0(2^{-j}\xi),$$

$$\hat{\tilde{\phi}}(\xi) = (2\pi)^{-1/2} \prod_{j=1}^{\infty} \tilde{m}_0(2^{-j}\xi),$$

$$\hat{\psi}(\xi) = e^{-i\xi/2}\overline{\tilde{m}_0(\xi/2 + \pi)}\hat{\phi}(\xi/2),$$

$$\hat{\tilde{\psi}}(\xi) = e^{-i\xi/2}\overline{m_0(\xi/2 + \pi)}\hat{\tilde{\phi}}(\xi/2).$$

(Note that $\tilde{m}_0$ is used in the definition of ψ, and m_0 for $\tilde{\psi}$.) One has again that if some extra technical conditions are imposed on m_0, $\tilde{m}_0$, then the $\psi_{j,k}$ and the $\tilde{\psi}_{j,k}$ constitute Riesz bases for $L^2(\mathbb{R})$. They are dual bases; i.e.,

$$\langle \psi_{j,k}, \tilde{\psi}_{j',k'} \rangle = \delta_{j,j'}\delta_{k,k'}.$$

This duality is also reflected by the fact that

$$\psi_{j,k} \perp \tilde{V}_j, \quad \tilde{\psi}_{j,k} \perp V_j.$$

A more detailed exposition, with proofs and examples, can be found in Cohen *et al.* [8]; see also Cohen and Daubechies [4]. Symmetry for ϕ, ψ and $\tilde{\phi}$, $\tilde{\psi}$ is now possible because there exist symmetric solutions m_0, $\tilde{m}_0$ to (1.8). Two possibilities exist: if m_0, $\tilde{m}_0$ have an even number of coefficients, then $\phi(x)$ is symmetric around $x = 1/2$, and ψ is antisymmetric around the same point; if m_0 and $\tilde{m}_0$ have an odd number of coefficients, then ϕ and ψ are both symmetric, $\phi(x)$ around $x = 0$, $\psi(x)$ around $x = 1/2$.

Smoothness for these "biorthogonal" wavelet bases again requires a factorization similar to (1.7) for m_0 or $\tilde{m}_0$. More precisely, we now have

$$\psi \in C^k(\mathbb{R}) \Rightarrow \int dx\, x^l \tilde{\psi}(x) = 0 \quad l = 0, \ldots, k$$

$$\Updownarrow$$

$$\frac{d^l}{d\xi^l} m_0 \Big|_{\xi=\pi} = 0 \quad l = 0, \ldots, k,$$

which is again equivalent to a factorization of type (1.7) for m_0. Similarly, smoothness for $\tilde{\psi}$ requires zero moments for ψ, or a factorization similar to (1.7) for $\tilde{m}_0$.

All the above concerns bases for $L^2(\mathbb{R})$. (These one-dimensional constructions can easily be extended to higher dimensions, but we stick to one dimension here.) In many applications, however, one is interested in problems confined to an interval. Examples are numerical analysis (with boundary conditions at the edges of the interval) or image analysis (where the domain of interest is the Cartesian product of two intervals). To fix notations, let us assume that the interval is $[0, 1]$. It is very easy to restrict the Haar basis for $L^2(\mathbb{R})$ to a basis for $L^2([0, 1])$; starting from the collection $\{\phi_{0,k}; k \in \mathbb{Z}\} \cup \{\psi_{j,k}; j \leq 0, k \in \mathbb{Z}\}$, which is an orthonormal basis for $L^2(\mathbb{R})$, it suffices to take the restrictions of these functions to $[0, 1]$. Since every one of them is supported either in $[0, 1]$ or in $\mathbb{R} \setminus]0, 1[$, the collection that remains after all the functions with restriction 0 have been weeded out, i.e., $\{\phi_{0,0}\} \cup \{\psi_{j,k}; j \leq 0, 0 \leq k \leq 2^{|j|} - 1\}$, is an orthonormal Haar basis for $L^2([0, 1])$. Things are not so trivial when one starts from smoother wavelet bases on the line. In the examples (1.7), both ϕ and ψ have support width $2N - 1$. In order to avoid having to deal with the two edges of $[0, 1]$ at the same time, we can choose to start from the basis $\{\phi_{-j_0,k}; k \in \mathbb{Z}\} \cup \{\psi_{j,k}; j \leq -j_0, k \in \mathbb{Z}\}$ for $L^2(\mathbb{R})$, where j_0 is chosen large enough so that none of the functions has support straddling both 0 and 1 (i.e., $2^{j_0 - 1} \geq N$). Even so there will be $2N - 2$ functions, at every resolution level and at every end of $[0, 1]$, among these orthonormal basis functions, that straddle an endpoint, so that their support is neither completely in $[0, 1]$ nor completely in $\mathbb{R} \setminus]0, 1[$. It is not a priori clear how to adapt them in such a way that the result is an orthonormal basis of $L^2([0, 1])$.

Several solutions have been proposed for this problem. They all correspond to different choices of how to adapt the multiresolution hierarchy to the interval $[0, 1]$.

A first solution consists in not doing anything at all. A function f supported on $[0, 1]$ can always be extended to the whole line by putting $f(x) = 0$ for $x \notin [0, 1]$. This function can then be analyzed by means of the wavelets on the whole real line. There are two things wrong with this naive approach. First of all, this kind of extension typically introduces a discontinuity in f at $x = 0$ or 1, which is reflected by "large" wavelet coefficients for fine scales (i.e., wavelet coefficients which do not decay very fast) near the two edges, even if f itself is very smooth on $[0, 1]$. The (one-sided) regularity of f at 0 or 1 is therefore not characterized by the decay of the $\langle f, \psi_{j,k} \rangle$ for $j \to -\infty$. The second "bad" aspect is that this approach uses "too many" wavelets. At scale $-j$, one finds $\langle f, \psi_{-j,k} \rangle \neq 0$ for the typically $2^j + 2N - 1$ wavelets corresponding to $-(2N - 2) \leq k \leq 2^j - 1$; intuitively one should have to use only 2^j wavelets, at scale $-j$, when looking at problems on $[0, 1]$. We shall come back to this *desirability* of having exactly 2^j wavelets.

A second solution consists in periodizing. In this case, one expands a function f on $[0, 1]$ into "periodized" wavelets defined by

$$\psi^{\text{per}}_{-j,k}(x) = 2^{j/2} \sum_{l \in \mathbb{Z}} \psi(2^j x + 2^j l - k),$$

with $j \geq j_0 \geq 0$ (for $j < 0$, the $\psi^{\text{per}}_{-j,k}$ vanish identically), $0 \leq k \leq 2^j - 1$. These wavelets have to be supplemented by lowest resolution scaling functions $\phi^{\text{per}}_{-j_0,k}$, defined analogously; the result is an orthonormal basis of $L^2([0, 1])$, associated with a multiresolution analysis in which V^{per}_{-j} is spanned by the $\phi^{\text{per}}_{-j,k}$. In this case, one has indeed exactly 2^j wavelets at scale $-j$; the number of scaling functions $\phi^{\text{per}}_{-j,k}$ in every V^{per}_{-j} is also 2^j. Since obviously

$$\int_0^1 dx f(x) \psi^{\text{per}}_{-j,k}(x) = \int_{-\infty}^{\infty} dx \, [\sum_l f(x + l)] \psi_{-j,k}(x),$$

expanding a function on $[0, 1]$ into periodized wavelets is equivalent to extending the original function into a periodic function with period 1 and analyzing this extension with the standard whole-line wavelets. It follows that, unless f itself was already periodic, this construction introduces again a discontinuity at $x = 0$, $x = 1$, which shows up as slow decay in the fine scale wavelet coefficients pertaining to the edges. Again, it is impossible to characterize the one-sided regularity of f at 0 or 1 by simply looking at the decay of the $|\langle f, \psi^{\text{per}}_{j,k} \rangle|$ for $j \to -\infty$, unless f is periodic.

A third solution, often adopted in image analysis, is to reflect at the edges. In this case, one extends the function f on $[0, 1]$ by mirroring it at 0 and 1:

$$f(x) = f(2 - x) \quad \text{for} \quad 1 \leq x \leq 2$$
$$f(x) = f(-x) \quad \text{for} \quad -1 \leq x \leq 0.$$

Beyond -1 and 2 we mirror once more, and so on. The full extension is then defined by

$$\begin{aligned} f(x) &= f(2n - x) \quad 2n - 1 \leq x \leq 2n \\ &\quad f(x - 2n) \quad 2n \leq x \leq 2n + 1. \end{aligned} \tag{1.9}$$

If the original function on $[0, 1]$ is continuous at 0 and 1, then this extension is continuous at all the integers. Typically, however, the derivative of the extension has discontinuities at the integers. Expanding the extension (1.9) of a function f on $[0, 1]$ in a whole-line basis of wavelets is equivalent to expanding the original function on $[0, 1]$ with respect to the "folded" wavelets $\psi_{j,k}^{\text{fold}}$ defined on $[0, 1]$ by

$$\psi_{j,k}^{\text{fold}}(x) = \sum_{l \in \mathbb{Z}} \psi_{j,k}(x - 2l) + \sum_{l \in \mathbb{Z}} \psi_{j,k}(2l - x).$$

Starting from an orthonormal wavelet basis, this folding typically does not lead to an orthonormal wavelet basis on $[0, 1]$. If ψ_{jk}, $\tilde{\psi}_{jk}$ are two biorthogonal wavelet bases, with ψ and $\tilde{\psi}$ both symmetric or antisymmetric around $1/2$, then their folded versions are still biorthogonal on $[0, 1]$, however. We discuss this in some more detail in Section 2, with examples. The resulting biorthogonal multiresolution analysis hierarchies on $[0, 1]$ have $2^j + 1$ (symmetric case) or 2^j (antisymmetric case) scaling functions and 2^j wavelets at resolution level j. Because the extension (1.9) typically has a discontinuous derivative, we again cannot expect to characterize arbitrary regularity of f by means of the wavelet coefficients; decay of the $\langle f, \psi_{jk}^{\text{fold}} \rangle$ can characterize up to Lipschitz regularity (a gain over the two previous "solutions"), but not more. (One can do a little better by using two different pairs of biorthogonal bases; see Section 2.)

A fourth solution was proposed in Meyer [21]. The starting point of this construction is any one of the compactly supported bases in Daubechies [9], with N vanishing moments, and support ψ = support $\phi = [0, 2N - 1]$. The basis on $[0, 1]$ constructed by Meyer is derived from a multiresolution analysis that "lives" on $[0, 1]$. At sufficiently fine scales, the approximation spaces $V_j^{[0,1]}$ consist of $2^j - 2N - 2$ "interior" functions, $2N - 2$ "left edge" functions, and $2N - 2$ "right edge" functions. The complement spaces $W_j^{[0,1]}$ are generated by $2^j - 2N - 2$ "interior" wavelets, $N - 1$ "left edge" wavelets, and $N - 1$ "right edge" wavelets. The total number of wavelets at scale j is thus 2^j, but the total number of scaling functions is larger, $2^j + 2N - 2$. The "interior" functions are simply ψ_{jk} or ϕ_{jk}, as they were defined on the whole line, for which the indices j, k happen to correspond to support ψ_{jk} or support $\phi_{jk} \subset [0, 1]$. The "edge" functions have to be constructed explicitly. The result of Meyer's construction is an orthonormal family of wavelets in $[0, 1]$, with N vanishing moments, and the same regularity as the original ψ; together with an orthonormal family of scaling functions on $[0, 1]$ at the coarsest scale under consideration, these adapted wavelets constitute an orthonormal basis for $L^2([0, 1])$. In addition, their regularity and vanishing moment properties ensure that they are unconditional wavelet bases for the Hölder spaces $C^s([0, 1])$ for all $s < r$, where r is the regularity of the original wavelet basis, $\psi \in C^r$. We recapitulate in Section 3 the main steps of Meyer's construction (very briefly, without proofs), and give tables for the corresponding adapted "filter" coefficients near the edges. Meyer's construction has two weaknesses. Because the number of scaling functions at resolution j is larger than the number of wavelets, the construction cannot be generalized to wavelet packets on the interval: in a wavelet packet construction, wavelet coefficients get split as well as scaling coefficients, using the same filters, and for this it is essential that the two families have the same number of coefficients at every scale. The fact that the number of scaling functions is not a power of 2 is also a nuisance for practical applications such as image analysis, where arrays are typically squares with 256×256 or 512×512 pixels. The other objection to Meyer's construction is that the explicit construction of the edge functions involves the diagonalization of a matrix that becomes ill conditioned for reasonably large N. We shall discuss this in more detail in Section 3.

This paper presents a fifth solution, also derived from compactly supported wavelet bases for $\mathbb{R}$. Like Meyer's solution, it uses "interior" and "edge" scaling functions at every resolution. We introduce fewer edge functions, however, tailoring them so that the total number is exactly 2^j at resolution j; moreover, as in Meyer's case, all the polynomials on $[0, 1]$ of degree $\leq N - 1$ can be written as linear combinations of the scaling functions at any fixed scale. It then follows that all the corresponding wavelets, at the edge as well as in the interior, have N vanishing moments, and this is sufficient to ensure that we again have unconditional bases for the $C^s([0, 1])$-spaces, with $s < r$ if $\psi \in C^r$. This new construction is explained in detail in Section 4, with many examples and consequences. After completing this work, we learned that a similar construction was made independently by Jouini and Lemarié-Rieusset [16], and by B. Jawerth. A first announcement of the results was made jointly by B. Jawerth and the present authors in [5]; extensions and applications (developed independently of this paper) can be found in L. Andersson *et al.* [1].

2. FOLDING BIORTHOGONAL WAVELETS

Given any reasonably decaying function f on $\mathbb{R}$, we define its "folded" version by

$$f^{\text{fold}}(x) = \sum_{n \in \mathbb{Z}} [f(x - 2n) + f(2n - x)]. \quad (2.1)$$

This function has the property that, for all $x \in \mathbb{R}$, $k \in \mathbb{Z}$,

$$f^{\text{fold}}(-x) = f^{\text{fold}}(x)$$
$$f^{\text{fold}}(x + 2k) = f^{\text{fold}}(x). \quad (2.2)$$

For later convenience, note that

$$\int_0^1 dx f^{\text{fold}}(x) g^{\text{fold}}(x) = \int_{-\infty}^{\infty} dx f(x) g^{\text{fold}}(x), \quad (2.3)$$

an easy consequence of (2.2).

Suppose now that $\psi, \tilde{\psi}$ are two compactly supported wavelets giving rise to biorthogonal wavelet bases, with associated scaling functions $\phi, \tilde{\phi}$ and multiresolution analyses $\cdots \subset V_1 \subset V_0 \subset V_{-1} \subset \cdots$, $\cdots \subset \tilde{V}_1 \subset \tilde{V}_0 \subset \tilde{V}_{-1} \subset \cdots$, as in Cohen *et al.* [8]. We "fold" these wavelets and scaling functions and study the result. This is interesting only if we can exploit symmetries of ϕ, ψ, $\tilde{\phi}$, and $\tilde{\psi}$, and we therefore assume that these functions have symmetry axes. There are two cases to distinguish: either $\phi(x) = \phi(1 - x)$, $\psi(x) = -\psi(1 - x)$ (same for $\tilde{\phi}, \tilde{\psi}$), corresponding to an even number of non-zero taps in the filters m_0 and $\tilde{m}_0$, or $\phi(x) = \phi(-x)$, $\psi(1 - x) = \psi(x)$ (same for $\tilde{\phi}, \tilde{\psi}$), with an odd number of non-zero taps in the filters m_0 and $\tilde{m}_0$. We start by considering the first case, where $\phi, \tilde{\phi}$ are symmetric and $\psi, \tilde{\psi}$ are antisymmetric around $1/2$. The corresponding m_0, $\tilde{m}_0$ are then necessarily of the type

$$m_0(\xi) = \left(\frac{1 + e^{-i\xi}}{2}\right)\left(\cos^2\frac{\xi}{2}\right)^l p\left(\sin^2\frac{\xi}{2}\right)$$
$$\tilde{m}_0(\xi) = \left(\frac{1 + e^{-i\xi}}{2}\right)\left(\cos^2\frac{\xi}{2}\right)^{\tilde{l}} \tilde{p}\left(\sin^2\frac{\xi}{2}\right)$$

with $p, \tilde{p}$ two polynomials such that

$$x^{l+\tilde{l}+1} p(1 - x)\tilde{p}(1 - x) + (1 - x)^{l+\tilde{l}+1} p(x)\tilde{p}(x) = 1.$$

Several examples are given in Cohen *et al.* [8]; in addition C. Brislawn has drawn our attention to examples in which m_0 and $\tilde{m}_0$ have the same number of "taps" (i.e., the same number of non-zero coefficients when written out as polynomials in $e^{-i\xi}$). The wavelets $\psi, \tilde{\psi}$ can be made arbitrarily regular by choosing $l, \tilde{l}$ large enough, and picking appropriate $p, \tilde{p}$.

Define the space V_j^{fold} to be the closed linear span of the $\phi_{j,k}^{\text{fold}}$, $k \in \mathbb{Z}$, where the closure is taken with respect to $L^2([0, 1])$. (Because of (2.2), any linear combination of $\phi_{j,k}^{\text{fold}}$ is completely determined by its restriction to $[0, 1]$, so that we can identify the linear span of the $\phi_{j,k}^{\text{fold}}$ with a subspace of $L^2([0, 1])$.) Spaces $\tilde{V}_j^{\text{fold}}$, W_j^{fold}, and $\tilde{W}_j^{\text{fold}}$ are defined analogously. As in the periodized case (see Meyer [20]), these spaces are non-trivial only for sufficiently fine resolution. For $j \geq 2$ we have that

$$\psi_{j,k}^{\text{fold}}(x) = 2^{-j/2} \sum_n [\psi(2^{-j}x - 2^{-j+1}n - k) + \psi(-2^{-j}x + 2^{-j+1}n - k)] = 0$$

because $\Sigma_l \psi(x - l/2) = 0$ (a consequence of $\psi(x) = \sqrt{2} \times \Sigma_n g_n \phi(2x - n)$, with $\Sigma_n g_n = 0$, $\Sigma_k \phi(x - k) = 1$). For $j = 1$, we use $\psi(x) + \psi(1 - x) = 0$ to conclude that

$$\psi_{1,k}^{\text{fold}}(x) = 2^{-1/2} \sum_n \left[\psi\left(\frac{x}{2} - n - k\right) + \psi\left(-\frac{x}{2} + n - k\right)\right]$$
$$= 2^{-1/2} \sum_m \left[\psi\left(\frac{x}{2} - m\right) - \psi\left(\frac{x}{2} + m + 1\right)\right] = 0.$$

It follows that $W_j^{\text{fold}} = \{0\}$ for $j \geq 1$; similarly $\tilde{W}_j^{\text{fold}} = \{0\}$ for $j \geq 1$. On the other hand $\Sigma_k \phi(x - k) = 1$ implies, for $j \geq 1$, that

$$\phi_{j,k}^{\text{fold}}(x) = 2^{-j/2} \sum_n [\phi(2^{-j}x - 2^{-j+1}n - k) + \phi(-2^{-j}x + 2^{-j+1}n - k)] = 2^{j/2},$$

whereas, for $j = 0$, $\phi(x) = \phi(1 - x)$ leads to

$$\phi_{0,k}^{\text{fold}}(x) = \sum_n [\phi(x - 2n - k) + \phi(-x + 2n - k)]$$
$$= \sum_n [\phi(x - 2n - k) + \phi(x - 2n + k + 1)]$$
$$= \sum_m \phi(x + m) = 1.$$

It follows that the V_j^{fold} (and $\tilde{V}_j^{\text{fold}}$) spaces collapse to only the constant functions if $j \geq 0$. We therefore consider the folded spaces only for $j \leq 0$. For $j = -J \leq 0$, the equations (2.2) imply that

$$\phi_{-J,k+2^{J+1}m}^{\text{fold}} = \phi_{-J,k}^{\text{fold}} \quad (2.4)$$

and

$$\phi_{-J,2^{J+1}-k-1}^{\text{fold}} = \phi_{-J,k}^{\text{fold}}, \quad (2.5)$$

so that we can restrict ourselves to $k = 0, \ldots, 2^J - 1$. The same happens with $\tilde{\phi}$, ψ, $\tilde{\psi}$ (with a change of sign in (2.4) for $\psi, \tilde{\psi}$).

It turns out that the $\phi_{-J,k}^{\text{fold}}$, $\tilde{\phi}_{-J,k'}^{\text{fold}}$, $0 \leq k, k' \leq 2^J - 1$, inherit the biorthogonality of the unfolded versions, as can be seen by using (2.3):

$$\int_0^1 dx \phi^{\text{fold}}_{-J,k}(x)\overline{\tilde{\phi}^{\text{fold}}_{-J,k'}(x)}$$

$$= \sum_{n\in\mathbb{Z}} [\langle \phi_{-J,k}, \tilde{\phi}_{-J,k'+2^{J+1}n}\rangle + \langle \phi_{-J,k}, \tilde{\phi}_{-J,2^{J+1}n-k'-1}\rangle]$$

$$= \sum_{n\in\mathbb{Z}} [\delta_{k,k'+2^{J+1}n} + \delta_{k,2^{J+1}n-k'-1}] = \delta_{k,k'}.$$

This biorthogonality implies, among other things, that the $\phi^{\text{fold}}_{-J,k}$, $k = 0, \ldots, 2^J - 1$ are all independent, so that V^{fold}_{-J} is a 2^J-dimensional space. Completely analogously, we can derive

$$\int_0^1 dx \psi^{\text{fold}}_{-J,k}(x)\overline{\tilde{\phi}^{\text{fold}}_{-J,k'}(x)} = 0 = \int_0^1 dx \tilde{\psi}^{\text{fold}}_{-J,k}(x)\overline{\phi^{\text{fold}}_{-J,k}(x)}$$

$$\int_0^1 dx \psi^{\text{fold}}_{-J,k}(x)\overline{\tilde{\psi}^{\text{fold}}_{-J,k'}(x)} = \delta_{k,k'},$$

proving that $W^{\text{fold}}_{-J} \perp \tilde{V}^{\text{fold}}_{-J}$, $\tilde{W}^{\text{fold}}_{-J} \perp V^{\text{fold}}_{-J}$, and that the $\psi^{\text{fold}}_{-J,k}$, $k = 0, \ldots, 2^J - 1$ constitute a basis for the 2^J-dimensional space W^{fold}_{-J}.

In summary, we have two ladders

$$V^{\text{fold}}_0 \subset V^{\text{fold}}_{-1} \subset V^{\text{fold}}_{-2} \subset \cdots$$

(same for the $\tilde{V}^{\text{fold}}_j$) of nested 2^j dimensional spaces V^{fold}_{-j}, and 2^j-dimensional complement spaces W^{fold}_{-j}, $j \geq 0$, with

$$V^{\text{fold}}_{-j} \oplus W^{\text{fold}}_{-j} = V^{\text{fold}}_{-j-1}$$

(where the direct sum is not orthogonal). In addition, we have the biorthogonality relations proved above, linking the two hierarchies. Moreover $V^{\text{fold}}_0 = \tilde{V}^{\text{fold}}_0$ consists of only the constant functions, and one easily derives $\overline{\cup_{j=0}^{\infty} V^{\text{fold}}_{-j}} = \overline{\cup_{j=0}^{\infty} \tilde{V}^{\text{fold}}_{-j}} = L^2([0,1])$ from the analogous relation for the unfolded spaces. Any $f \in L^2(\mathbb{R})$ can therefore be written as

$$f = \langle f, \tilde{\phi}^{\text{fold}}_{0,0}\rangle \phi^{\text{fold}}_{0,0} + \lim_{J\to\infty} \sum_{j=0}^{J} \sum_{k=0}^{2^j-1} \langle f, \tilde{\psi}^{\text{fold}}_{-j,k}\rangle \psi^{\text{fold}}_{-j,k}$$

$$= \sum_{k=0}^{2^L-1} \langle f, \tilde{\phi}^{\text{fold}}_{-L,k}\rangle \phi^{\text{fold}}_{-L,k} + \lim_{J\to\infty} \sum_{j=L}^{J} \sum_{k=0}^{2^j-1} \langle f \tilde{\psi}^{\text{fold}}_{-j,k}\rangle \psi^{\text{fold}}_{-j,k}.$$

This is not sufficient to ensure that the $\{\phi^{\text{fold}}_{-L,k}, k = 0, \ldots, 2^L - 1\} \cup \{\psi^{\text{fold}}_{-j,k}; j \geq L, k = 0, \ldots, 2^j - 1\}$ constitute a Riesz basis, however. (See the similar discussion in Cohen *et al.* [8].) We still need to establish frame bounds. To show how the folded wavelets inherit frame bounds from their unfolded parents we exploit that $\psi, \tilde{\psi}$ are compactly supported. (An only slightly less trivial argument can handle the case where $\psi, \tilde{\psi}$ are not compactly supported but have good decay.) If support $\psi = [-K+1, K]$ (remember that ψ has a symmetry axis at $x = 1/2$), then support $\psi_{-j,k} = [(k-K+1)2^{-j}, (K+k)2^{-j}]$, so that $\psi^{\text{fold}}_{-j,k}(x) = \psi_{-j,k}(x)$ for $0 \leq x \leq 1$ if $2K - 1 \leq 2^j$ and $K - 1 \leq k \leq 2^j - K$. If $2^j \geq 2K - 1$ but $0 \leq k < K - 1$, then $\psi^{\text{fold}}_{-j,k}(x) = \psi_{-j,k}(x) - \psi_{-j,-k-1}(x)$ for $0 \leq x \leq 1$; similarly $\psi^{\text{fold}}_{-j,k}(x) = \psi_{-j,k}(x) - \psi_{-j,2^{j+1}+1-k}(x)$ for $0 \leq x \leq 1$ and $2^j - K < k \leq 2^j - 1$. Now take $f \in L^2([0,1])$ and define its extension to all of $\mathbb{R}$ by $f^{\text{ext}}(x) = f(x)$ for $x \in [0,1]$, $f^{\text{ext}}(x) \equiv 0$ for $x \notin [0,1]$. Define j_0 to be the smallest j such that $2^j \geq 2K - 1$. Then

$$\sum_{j=j_0}^{\infty} \sum_{k=0}^{2^j-1} |\langle f, \psi^{\text{fold}}_{-j,k}\rangle|^2$$

$$= \sum_{j=j_0}^{\infty} [\sum_{k=0}^{K-2} |\langle f^{\text{ext}}, \psi_{-j,k}\rangle - \langle f^{\text{ext}}, \psi_{-j,-k-1}\rangle|^2$$

$$+ \sum_{k=K-1}^{2^j-K} |\langle f^{\text{ext}}, \psi_{-j,k}\rangle|^2$$

$$+ \sum_{k=2^j-K+1}^{2^j-1} |\langle f^{\text{ext}}, \psi_{-j,k}\rangle - \langle f^{\text{ext}}, \psi_{-j,2^{j+1}+1-k}\rangle|^2]$$

$$\leq 2 \sum_{j=j_0}^{\infty} \sum_{k=-K+1}^{2^j+K} |\langle f^{\text{ext}}, \psi_{-j,k}\rangle|^2$$

$$= 2 \sum_{j=j_0}^{\infty} \sum_{k=-\infty}^{\infty} |\langle f^{\text{ext}}, \psi_{-j,k}\rangle|^2, \tag{2.8}$$

where we have used in the final step that support $\psi_{-j,k} \cap [0,1] = \varnothing$ for $k \leq -K$ or $k \geq 2^j + K + 1$. The frame bounds for the $\psi_{j,k}$ on the whole line then imply that (2.8) is bounded by $2B \int_{-\infty}^{\infty} dx\, |f^{\text{ext}}(x)|^2 = 2B \int_0^1 dx\, |f(x)|^2$, for some $B < \infty$. Since there are only finitely many $\psi^{\text{fold}}_{-j,k}$ to be considered for $j < j_0$, this proves that, for all $f \in L^2([0,1])$,

$$|\langle f, \phi^{\text{fold}}_{0,0}\rangle|^2 + \sum_{j=0}^{\infty} \sum_{k=0}^{2^j-1} |\langle f, \psi^{\text{fold}}_{-j,k}\rangle|^2 \leq B' \|f\|^2,$$

for some $B' < \infty$. The same is true for the $\tilde{\phi}^{\text{fold}}$, $\tilde{\psi}^{\text{fold}}$, and the two upper bounds together with the duality (2.6) lead to lower frame bounds, by Cauchy–Schwarz.

For numerical implementation in the $L^2(\mathbb{R})$ case, one uses the filter coefficients c_n, or rather $h_n = \sqrt{2}c_n$, from (1.1), and the $\tilde{h}_n$ corresponding to $\tilde{m}_0$, rather than $\phi, \psi, \tilde{\phi}, \tilde{\psi}$ themselves. The filter coefficients to be used for the folded functions $\phi^{\text{fold}}, \cdots$ in the $L^2([0,1])$ case are simply correspondingly folded versions of the h_n and $g_n = (-1)^n h_{-n+1}$. From $\phi_{j,k}(x) = \Sigma_m h_m \phi_{-j-1,2k+m}(x)$ we immediately have

$$\phi^{\text{fold}}_{-j,k}(x) = \sum_m h_m \phi^{\text{fold}}_{-j-1,2k+m}(x)$$

$$= \sum_l h_{l-2k} \phi^{\text{fold}}_{-j-1,l}(x). \tag{2.9}$$

If support $\phi = [-L+1, L]$, then $h_m \equiv 0$ for $m \leq -L$ or $m > L$, so that formula (2.9) can be adopted as is for $(L-1)/2 \leq k \leq 2^j - (L-1)/2$. For k outside this range, the index $2k+m$ may fall outside $\{0, 1, \ldots, 2^{j+1}-1\}$, and we need to apply (2.4), (2.5). For $0 \leq k < (L-1)/2$, for instance,

$$\begin{aligned}\phi^{\text{fold}}_{-j,k} &= \sum_{m=-2k}^{L} h_m \phi^{\text{fold}}_{-j-1,2k+m} \\ &\quad + \sum_{m=-L+1}^{-2k-1} h_m \phi^{\text{fold}}_{-j-1,-2k-m-1} \\ &= \sum_{l \geq 0} (h_{l-2k} + h_{-2k-l-1}) \phi^{\text{fold}}_{-j-1,l}. \qquad (2.10)\end{aligned}$$

Something similar happens for $2^j - (L-1)/2 < k \leq 2^j - 1$; if $2^j < (L-1)$, then even more folding terms step in, because the two edges come into play simultaneously. Similar formulas can be derived for the high-pass filters linking the $\psi^{\text{fold}}_{-j,k}$ with $\phi^{\text{fold}}_{-j-1,l}$. This finishes our discussion of the case where ϕ, $\tilde{\phi}$ and ψ, $\tilde{\psi}$ both have their symmetry axes at $x = 1/2$. We end up with a multiresolution analysis with exactly 2^j functions in the jth approximation space as well as in the jth wavelet space, which means that these can be used for wavelet packet constructions as well. Moreover, it is easy to find the "folded" filter coefficients from the original ones; Fig. 1 illustrates how the coefficients near the edge are affected in a simple case.

Let us now consider the case where ϕ, $\tilde{\phi}$ have a symmetry axis at $x = 0$, $\phi(x) = \phi(-x)$, $\tilde{\phi}(x) = \tilde{\phi}(-x)$, and ψ, $\tilde{\psi}$ are symmetric around $x = 1/2$, $\psi(1-x) = \psi(x)$, $\tilde{\psi}(1-x) = \tilde{\psi}(x)$. This corresponds to an odd number of non-zero coefficients in m_0, $\tilde{m}_0$; more precisely, m_0, $\tilde{m}_0$ are of the type

$$m_0(\xi) = \left(\cos^2 \frac{\xi}{2}\right)^l p\left(\sin^2 \frac{\xi}{2}\right),$$

$$\tilde{m}_0(\xi) = \left(\cos^2 \frac{\xi}{2}\right)^{\tilde{l}} \tilde{p}\left(\sin^2 \frac{\xi}{2}\right),$$

with

$$x^{l+\tilde{l}} p(1-x)\tilde{p}(1-x) + (1-x)^{l+\tilde{l}} p(x)\tilde{p}(x) = 1.$$

There are again several examples in Cohen *et al.* [8], including some examples where ϕ and $\tilde{\phi}$ are very "close." There exist no examples with the same number of non-vanishing coefficients for both m_0 and $\tilde{m}_0$ in this case.

Define the folded scaling functions, the wavelets, and the spaces they generate as before. One now checks that

$$\begin{aligned}\psi^{\text{fold}}_{j,k} &\equiv 0 \quad &&\text{if} \quad &&j \geq 2 \\ \psi^{\text{fold}}_{1,k} &= \psi^{\text{fold}}_{1,0} \quad &&\text{for all} \quad &&k \in \mathbb{Z} \\ \Phi^{\text{fold}}_{j,k} &= 2^{j/2} \quad &&\text{if} \quad &&j \geq 1.\end{aligned}$$

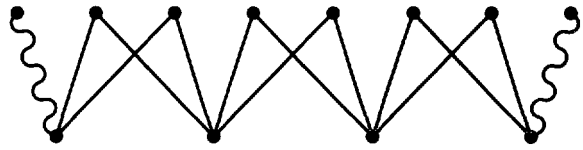

FIG. 1. Low pass filtering scheme for the "folded" case, going from V^{fold}_{-3} to V^{fold}_{-2}, in the case where support $\phi = [-1, 2]$, i.e., only h_{-1}, h_0, h_1, h_2 are $\neq 0$; in fact $h_0 = h_1 = \alpha$, $h_{-1} = h_2 = \beta$ because of the symmetry conditions imposed (see text). The straight lines represent unaffected filter coefficients. In this case only two filter coefficients are affected by the folding (wavy lines—one at each end); the folded coefficient here is $h_0 + h_{-1} = h_0 + h_2$.

For $j = -J \leq 0$, one has

$$\phi^{\text{fold}}_{-J,k} = \sum_n [\phi_{-J,k+2^{J+1}n} + \phi_{-J,2^{J+1}n-k}]$$

$$\psi^{\text{fold}}_{-J,k} = \sum_n [\psi_{-J,k+2^{J+1}n} + \psi_{-J,2^{J+1}n-k-1}].$$

Similar equations hold for $\tilde{\phi}$, $\tilde{\psi}$; all the derivations are analogous to the previous case. It follows that we now restrict ourselves to the V^{fold}_{-j}, W^{fold}_{-j} spaces (and their $\tilde{}$ equivalents) for $j \geq -1$ (as opposed to $j \geq 0$ in the previous case). For $j \geq 0$,

$$\phi^{\text{fold}}_{-j,k+2^{j+1}m} = \phi^{\text{fold}}_{-j,k} \quad \text{and} \quad \phi^{\text{fold}}_{-j,2^{j+1}-k} = \phi^{\text{fold}}_{-j,k},$$

$$\psi^{\text{fold}}_{-j,k+2^{j+1}m} = \psi^{\text{fold}}_{-j,k} \quad \text{and} \quad \psi^{\text{fold}}_{-j,2^{j+1}-k-1} = \psi^{\text{fold}}_{-j,k}$$

(same for $\tilde{\phi}$, $\tilde{\psi}$), implying that

$$\begin{aligned}\dim V^{\text{fold}}_{-j} &= \dim \tilde{V}^{\text{fold}}_{-j} = 2^j + 1, \\ \dim W^{\text{fold}}_{-j} &= \dim \tilde{W}^{\text{fold}}_{-j} = 2^j, \qquad (2.11)\end{aligned}$$

at least for $j \geq 0$. For $j = -1$, we have $\dim V^{\text{fold}}_1 = 1 = \dim \tilde{V}^{\text{fold}}_1$, $\dim W^{\text{fold}}_1 = 1 = \dim \tilde{W}^{\text{fold}}_1$. The independent basis functions in V^{fold}_{-j} can be taken as $\phi^{\text{fold}}_{-j,k}$, $k = 0, 1, \ldots, 2^j$; in W^{fold}_{-j} we take $\psi^{\text{fold}}_{-j,k}$, $k = 0, 1, \ldots, 2^j - 1$.

As in the previous case, one easily checks that

$$\int_0^1 dx \psi^{\text{fold}}_{-j,k}(x) \overline{\tilde{\psi}^{\text{fold}}_{-j,k'}(x)} = \delta_{k,k'}$$

$$\int_0^1 dx \psi^{\text{fold}}_{-j,k}(x) \overline{\tilde{\phi}^{\text{fold}}_{-j,k'}(x)} = 0 = \int_0^1 dx \tilde{\psi}^{\text{fold}}_{-j,k}(x) \overline{\phi^{\text{fold}}_{-j,k'}(x)}.$$

The biorthogonality of the ϕ, $\tilde{\phi}$ is slightly different:

$$\begin{aligned}\int_0^1 dx \phi^{\text{fold}}_{-j,k}(x) \overline{\tilde{\phi}^{\text{fold}}_{-j,k'}(x)} &= \int_{-\infty}^{\infty} dx \phi_{-j,k}(x) \overline{\phi^{\text{fold}}_{-j,k'}(x)} \\ &= \sum_n [\delta_{k,k'+2^{j+1}n} + \delta_{k,2^{j+1}n-k'}].\end{aligned}$$

If $0 < k < 2^j$, then this still equals $\delta_{k,k'}$, but for $k = 0$ or $k = 2^j$, we find $2\delta_{k,k'}$. In order to preserve biorthogonality, we are therefore forced to readjust the normalizations of $\phi^{\text{fold}}_{-j,0}$ and $\phi^{\text{fold}}_{-j,2^j}$ by defining

$$\phi^{\text{fold,n}}_{-j,0} = \frac{1}{\sqrt{2}}\phi^{\text{fold}}_{-j,0}, \quad \phi^{\text{fold,n}}_{-j,2^j} = \frac{1}{\sqrt{2}}\phi^{\text{fold}}_{-j,2^j}.$$

(The extra "n" stands for "normalized.") The same has to be done for $\tilde{\phi}^{\text{fold}}_{-j,0}$, $\tilde{\phi}^{\text{fold}}_{-j,2^j}$. For $j = -1$ we also redefine

$$\phi^{\text{fold,n}}_{1,0} \equiv 1 \equiv \tilde{\phi}^{\text{fold,n}}_{1,0}.$$

All the other scaling functions remain untouched; i.e.,

$$\phi^{\text{fold,n}}_{-j,k} \equiv \phi^{\text{fold}}_{-j,k} \quad \text{for} \quad j \geq 0, \quad 0 < k < 2^j.$$

We can then write, for any $f \in L^2([0, 1])$,

$$\begin{aligned} f &= \langle f, \tilde{\phi}^{\text{fold,n}}_{1,0}\rangle \phi^{\text{fold,n}}_{1,0} + \langle f, \tilde{\psi}^{\text{fold}}_{1,0}\rangle \psi^{\text{fold}}_{1,0} \\ &\quad + \sum_{j=0}^{\infty}\sum_{k=0}^{2^j-1} \langle f, \tilde{\psi}^{\text{fold}}_{-j,k}\rangle \psi^{\text{fold}}_{-j,k} \\ &= \sum_{k=0}^{2^L} \langle f, \tilde{\phi}^{\text{fold,n}}_{-L,k}\rangle \phi^{\text{fold,n}}_{-L,k} + \sum_{j=L}^{\infty}\sum_{k=0}^{2^j-1} \langle f, \tilde{\psi}^{\text{fold}}_{-j,k}\rangle \psi^{\text{fold}}_{-j,k}, \end{aligned}$$

where we do indeed have dual frames. (The existence of frame bounds follows exactly as in the previous case.) For numerical implementation, one needs the corresponding low- and high-pass filters, which correspond again to folded versions of the original h_n, g_n, $\tilde{h}_n$, $\tilde{g}_n$. For instance, if support $\phi = [-L, L]$, then (2.9) can be used as is for $L/2 \leq k \leq 2^j - L/2$. For $0 \leq k < L/2$, we have

$$\phi^{\text{fold}}_{-j,k} = \sum_{l \geq 0} (h_{l-2k} + h_{-2k-l})\phi^{\text{fold}}_{-j-1,l}; \tag{2.12}$$

the recurrence for the $\phi^{\text{fold,n}}_{-j,k}$ then follows by an easy adjustment. Note that this adjustment is not even necessary: one can keep working with the $\phi^{\text{fold}}_{-j,k}$ as they are, provided that at the reconstruction stage, the two extremal scaling coefficients get halved systematically at every step as one climbs back up on the resolution ladder. Figure 2 illustrates how (2.12) affects the coefficients near the edge in a simple case.

This second case corresponds to what is sometimes done in image analysis when filters with an odd number of taps are used; the trick of halving the extremal scaling coefficients at the reconstruction stage is well known.

Remark. One can avoid some of the peculiarities of the low resolution spaces in this second construction by folding as $-1/2$, $1/2$ instead of at 0, 1. The folding map is then

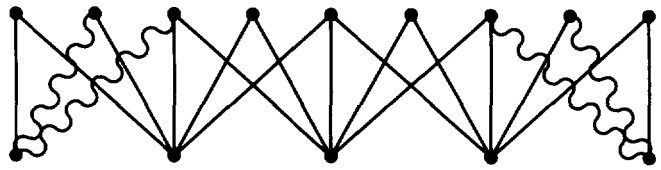

FIG. 2. Low pass filtering scheme for the "folded" case, going from V^{fold}_{-3} to V^{fold}_{-2}, in the case where support $\phi = [-2, 2]$, i.e., only h_{-2}, h_{-1}, h_0, h_1, h_2 are $\neq 0$; we have $h_{-2} = h_2$, $h_{-1} = h_1$ because of symmetry. This diagram corresponds to the unnormalized formula (2.12); some of the affected filter coefficients (wavy lines at edges) are equal to $\sqrt{2}$ times their normal value in this case.

$$f^{\text{fold},2}(x) = \sum_{n \in \mathbb{Z}} [f(x + 2n) + f(2n - x + 1)],$$

and one finds dim $V^{\text{fold},2}_j = 1$ for $j \geq 0$, so that only spaces with $j \leq 0$ need be considered. One still has dim $V^{\text{fold},2}_{-j} = 2^j + 1$ for $j \geq 1$, however.

To end this section, let us see for which values of s the coefficients $\langle f, \psi^{\text{fold}}_{-jk}\rangle$ can be used to characterize $f \in C^s([0, 1])$ in either of the two constructions. For $0 < s < 1$, we define $C^s([0, 1])$ by the straightforward definition

$$f \in C^s([0, 1]) \Leftrightarrow \|f\|_{C^s} = \sup\{|x - y|^{-s}|f(x) - f(y)|; \\ 0 \leq x, y \leq 1\} < \infty. \tag{2.13}$$

Suppose that ψ, $\phi \in C^r$, with $r > 1$. Then

PROPOSITION 2.1. *For $0 < s < 1$, a function f on $[0, 1]$ is in $C^s([0, 1])$ if and only if*

$$\sup_{\substack{j \geq 0 \\ 0 \leq k \leq 2^j - 1}} 2^{j(s+1/2)}|\langle f, \tilde{\psi}^{\text{fold}}_{-j,k}\rangle| < \infty. \tag{2.14}$$

Proof.

1. Assume first that $f \in C^s([0, 1])$. Because

$$\begin{aligned} \int_0^1 dx\, \tilde{\psi}^{\text{fold}}_{-j,k}(x) &= \sum_n \int_0^1 dx[\tilde{\psi}_{-j,k}(x + 2n) + \tilde{\psi}_{-j,k}(2n - x)] \\ &= \int_{-\infty}^{\infty} dx\, \tilde{\psi}_{-j,k}(x) = 0, \end{aligned}$$

we have

$$\begin{aligned} |\langle f, \tilde{\psi}^{\text{fold}}_{-j,k}\rangle| &= \left|\int_0^1 dx[f(x) - f(2^{-j}k)]\overline{\tilde{\psi}^{\text{fold}}_{-j,k}(x)}\right| \\ &\leq C\int_0^1 dx|x - 2^{-j}k|^s|\tilde{\psi}^{\text{fold}}_{-j,k}(x)|. \end{aligned} \tag{2.15}$$

We need to be concerned only about the behavior for large j. In that case, for most k, i.e., for $\tilde{K} - 1 \leq k \leq 2^j - \tilde{K}$ (where support $\tilde{\psi} = [-\tilde{K} + 1, \tilde{K}]$), support $\tilde{\psi}_{-j,k} \subset [0, 1]$, so that $\tilde{\psi}^{\text{fold}}_{-j,k}(x) = \tilde{\psi}_{-j,k}(x)$, and

$$(2.15) = C \int_{-\infty}^{\infty} dx |x - 2^{-j}k|^s |\tilde{\psi}_{-j,k}(x)|$$

$$= C \int_{-\infty}^{\infty} dx |x - 2^{-j}k|^s 2^{j/2} |\tilde{\psi}(2^j x - k)|$$

$$\leq C 2^{-j(s+1/2)} \int_{-\infty}^{\infty} dy |y|^s |\tilde{\psi}(y)|.$$

For $0 \leq k \leq \tilde{K} - 2$ we have

$$\tilde{\psi}^{\text{fold}}_{-j,k}(x) = \tilde{\psi}_{-j,k}(x) \pm \tilde{\psi}_{-j,-k-1}(x),$$

so that

$$(2.15) \leq C \int_0^{\infty} dx |x - 2^{-j}k|^s 2^{j/2} |\tilde{\psi}(2^j x - k)|$$

$$+ C \int_0^{\infty} dx |x - 2^{-j}k|^s 2^{j/2} |\tilde{\psi}(2^j x + k + 1)|$$

$$\leq 2C 2^{-j(s+1/2)} \int_{-\infty}^{\infty} dy |y|^s |\tilde{\psi}(y)|$$

$$+ C 2^{-js} |2k + 1|^s 2^{j/2} \int_{-\infty}^{\infty} dy |\tilde{\psi}(2^j y)|$$

$$\leq C' 2^{-j(s+1/2)}.$$

Something similar happens for $2^j - \tilde{K} + 1 \leq k \leq 2^j - 1$. This proves that (2.14) holds.

2. We now prove the converse. We have

$$|f(x) - f(y)| = |\sum_{j=0}^{\infty} \sum_{k=0}^{2^j - 1} \langle f, \tilde{\psi}^{\text{fold}}_{-j,k} \rangle [\psi^{\text{fold}}_{-j,k}(x)$$

$$- \psi^{\text{fold}}_{-j,k}(y)]| \leq C \sum_{j=0}^{\infty} \sum_{k=0}^{2^j - 1} 2^{-j(s+1/2)} |\psi^{\text{fold}}_{-j,k}(x) - \psi^{\text{fold}}_{-j,k}(y)|.$$

But

$$\psi^{\text{fold}}_{-j,k}(x) - \psi^{\text{fold}}_{-j,k}(y) = 2^{j/2} \{ \sum_n [\psi(2^j x - 2^{j+1} n - k)$$

$$- \psi(2^j y - 2^{j+1} n - k)] + \sum_n [\psi(2^{j+1} n - 2^j x - k)$$

$$- \psi(2^{j+1} n - 2^j y - k)] \};$$

together with $\psi(1 - x) = \pm \psi(x)$ this implies that

$$\sum_{k=0}^{2^j - 1} |\psi^{\text{fold}}_{-j,k}(x) - \psi^{\text{fold}}_{-j,k}(y)|$$

$$\leq 2^{j/2} \sum_{l=-\infty}^{\infty} |\psi(2^j x - l) - \psi(2^j y - l)|. \quad (2.16)$$

Because support $\psi \subset [-K + 1, K]$, at most $4K$ terms in this sum can contribute, so that

$$(2.16) \leq 4K 2^{j/2} \sup_l |\psi(2^j x - l) - \psi(2^j y - l)|$$

$$\leq C 2^{j/2} \min(1, 2^j |x - y|),$$

where we have used that ψ is bounded and Lipschitz. Consequently

$$|f(x) - f(y)|$$

$$\leq C \sum_{j=0}^{j_0} 2^{-js} 2^j |x - y| + C \sum_{j=j_0+1}^{\infty} 2^{-js}, \quad (2.17)$$

with j_0 determined by $2^{-j_0 - 1} < |x - y| \leq 2^{-j_0}$. This now immediately implies that

$$|f(x) - f(y)| \leq C' |x - y| 2^{j_0(1-s)}$$

$$+ C'' 2^{-j_0 s} \leq C''' |x - y|^s,$$

and $f \in C^s([0, 1])$. ▩

The arguments in this proof would not work for $s \geq 1$. For $s = 1$, the only problem is the very last step: the naive bound (2.17) would lead to an extra logarithmic factor in the bound on $|f(x) - f(y)|$, i.e., $|f(x) - f(y)| \leq C|x - y| \, |\log|x - y| \, |$. This can be avoided by replacing the Lipschitz space (obtained by taking $s = 1$ in (2.13)) with the larger space Λ_* of functions of Zygmund class. On the whole line $\Lambda_*(\mathbb{R})$ is defined by

$$\Lambda_*(\mathbb{R}) = \left\{ f : \mathbb{R} \to \mathbb{C}; \|f\|_{\Lambda_*} \right.$$

$$\left. = \sup_{x,h} \left| \frac{f(x + h) + f(x - h) - 2f(x)}{h} \right| < \infty \right\}; \quad (2.18)$$

as shown in Meyer [20],

$$f \in \Lambda_*(\mathbb{R}) \Leftrightarrow \sup_{j,k} 2^{3j/2} |\langle f, \psi_{-j,k} \rangle| < \infty.$$

If we restrict to $[0, 1]$, then the symmetric differences in (2.18) make no sense at $x = 0$ or 1; to define $\Lambda_*([0, 1])$ we

replace these symmetric differences by one-sided Lipschitz bound estimates at the edges 0 and 1 (for $x \in]0, 1[$ we keep the symmetric difference):

$$\Lambda_*([0,1]) = \left\{ f : [0,1] \to \mathbb{C}; \right.$$
$$\sup_{0 \leq x < y \leq 1} \left| \frac{f(x) + f(y) - 2f((x+y)/2)}{x - y} \right| < \infty,$$
$$\left. \sup_{1 \geq x > 0} \left| \frac{f(x) - f(0)}{x} \right| < \infty, \sup_{0 \leq y < 1} \left| \frac{f(1) - f(y)}{1 - y} \right| < \infty \right\}.$$

It is then still true that

PROPOSITION 2.2. *Let f be a bounded function on* $[0, 1]$. *Then*

$$f \in \Lambda_*([0,1]) \Leftrightarrow \sup_{\substack{j \geq 0 \\ 0 \leq k \leq 2^j - 1}} 2^{3j/2} |\langle f, \tilde{\psi}^{\text{fold}}_{-j,k} \rangle| < \infty. \quad (2.19)$$

Proof.

1. We start by extending f to all of $\mathbb{R}$ by defining

$$f^{\text{ext}}(x) = \begin{cases} f(x - 2n) & \text{if} \quad 2n \leq x \leq 2n + 1 \\ f(2n - x) & \text{if} \quad 2n - 1 \leq x \leq 2n. \end{cases} \quad (2.20)$$

This extension is an "unfolded" version of f, symmetric around every integer. It follows that $f \in \Lambda_*([0, 1]) \Leftrightarrow f^{\text{ext}} \in \Lambda_*(\mathbb{R})$.

2. On the other hand, for $j \geq 0$, $0 \leq k \leq 2^j - 1$,

$$\int_{-\infty}^{\infty} dx f^{\text{ext}}(x) \overline{\tilde{\psi}_{-j,k}(x)} = \int_0^1 dx f(x) \overline{\tilde{\psi}^{\text{fold}}_{-j,k}(x)}, \quad (2.21)$$

and, for all $n \in \mathbb{N}$,

$$\langle f^{\text{ext}}, \tilde{\psi}_{-j,k+2^{j+1}n} \rangle = \langle f^{\text{ext}}, \tilde{\psi}_{-j,k} \rangle$$
$$\langle f^{\text{ext}}, \tilde{\psi}_{-j,2^{j+1}n-k-1} \rangle = \pm \langle f^{\text{ext}}, \tilde{\psi}_{-j,k} \rangle.$$

Moreover $2^{-j/2} \langle f^{\text{ext}}, \tilde{\psi}_{j,k} \rangle$ is uniformly bounded for $j \geq 0$. It follows that

$$\sup_{j,k} 2^{3j/2} |\langle f^{\text{ext}}, \tilde{\psi}_{-j,k} \rangle| < \infty \Leftrightarrow$$
$$\sup_{\substack{j \geq 0 \\ 0 \leq k \leq 2^j - 1}} 2^{3j/2} |\langle f, \tilde{\psi}^{\text{fold}}_{-j,k} \rangle| < \infty.$$

3. The equivalence (2.19) now follows immediately from (2.21). ■

This takes care of $s = 1$; $s > 1$ is a different matter. Because of (2.21), and because the extension defined by (2.20) typically is only Lipschitz, even if f is very smooth on $[0, 1]$, we do not expect to be able to characterize $C^s([0, 1])$ spaces, with $s > 1$, by means of folded wavelet bases. (For $1 < s < 2$ we say that $f \in C^s([0, 1])$ if and only if f is differentiable on $]0, 1[$, left differentiable at 1, right differentiable at 0, and $\sup\{|x - y|^{-s} |f(x) - f(y) - f'(x)(x - y)|; 0 \leq x, y \leq 1\} < \infty$.) Let us have a closer look at how the proof of Proposition 2.1 fails when $s > 1$. First of all, in the argument in point 1, we replace $f(x)$ by $f(x) - f(2^{-j}k) - (x - 2^{-j}k) f'(2^{-j}k)$ in the evaluation of $\langle f, \tilde{\psi}^{\text{fold}}_{-j,k} \rangle$; to make the rest of the argument work, we require that $\int_0^1 dx\, x \tilde{\psi}^{\text{fold}}_{-j,k}(x) = 0$ for $0 \leq k \leq 2^j - 1$ and sufficiently large j. This is easily seen to be equivalent to $\int_0^\infty dx\, x \tilde{\psi}(x - m) = 0$, all $m \in \mathbb{Z}$ (look at sufficiently fine scales, and use $\int_{-\infty}^{\infty} dx\, x \tilde{\psi}(x) = 0$), which in turn is equivalent to $\times \int dx\, H(x) \tilde{\psi}(x - m) = 0$, all $m \in \mathbb{Z}$, where $H(x)$ is the hat function, $H(x) = 1 - |x|$ if $|x| \leq 1$, $H(x) = 0$ otherwise. One obvious construction of biorthogonal wavelet bases that satisfies this requirement is the case $m_0(\xi) = \cos^2(\xi/2)$; we have then $H(x) = \phi(x)$, which is necessarily orthogonal to all the $\tilde{\psi}(x - m)$. By playing around with the general recursion relations for $\tilde{\psi}$, $\tilde{\phi}$ as well as for H, one can also show that this is the only solution (see Appendix A). For these special biorthogonal wavelet bases where $\phi = H$ (and only for those!), one does therefore get decay $\sim 2^{-j(s+1/2)}$ for the $\langle f, \tilde{\psi}^{\text{fold}}_{-j,k} \rangle$ if $f \in C^s([0, 1])$ with $1 < s < 2$. (Higher values of s cannot be achieved.)

So much for the necessity part of condition (2.14). What about the sufficiency? To prove that $|f(x + t) - f(x) - f'(x)t| \leq C|t|^s$, with $1 < s < 2$, we would follow essentially the same procedure as in step 2 of the proof of Proposition 2.1, using the bound

$$|\psi^{\text{fold}}_{-j,k}(x + t) - \psi^{\text{fold}}_{-j,k}(x) - (\psi^{\text{fold}}_{-j,k})'(x)t| \leq C 2^{j/2} \min(1, (2^j |t|)^{1+r})$$

if $\psi \in C^{r+1}$. If $|\langle f, \tilde{\psi}^{\text{fold}}_{-j,k} \rangle| \leq C 2^{-j(s+1/2)}$, and $s < r + 1$, then the conclusion follows. Unfortunately, in the special biorthogonal bases where the necessary part of the theorem works, the wavelet ψ is a finite linear combination of hat functions, so that $\psi \notin C^{r+1}$ for $r > 0$. There is therefore, as we expected, no single biorthogonal wavelet basis construction for which $f \in C^s([0, 1])$ can be characterized by decay of the $\langle f, \tilde{\psi}^{\text{fold}}_{-j,k} \rangle$, if $s > 1$. However, the above argument shows that we *can* have a complete characterization of $C^s([0, 1])$ spaces with $1 < s < 2$, if we are willing to use two different pairs of biorthogonal bases, one pair ψ, $\tilde{\psi}$ for which $\phi = H$, and another pair Ψ, $\tilde{\Psi}$ such that Ψ is (say) C^2. Then

$$f \in C^s([0,1]) \Rightarrow |\langle f, \tilde{\psi}^{\text{fold}}_{-j,k} \rangle| \leq C 2^{-j(s+1/2)}$$

and

$$|\langle f, \tilde{\Psi}^{\text{fold}}_{-j,k} \rangle| \leq C 2^{-j(s+1/2)} \Rightarrow f \in C^s([0,1]).$$

3. THE ORTHONORMAL WAVELET BASES ON [0, 1] IN Y. MEYER'S CONSTRUCTION

We start by sketching the basic ideas in the Meyer [21] construction. At sufficiently small scales, the two edges of $[0, 1]$ "decouple" in the sense that wavelets or scaling functions near one edge are supported away from the other edge. One can therefore explain the idea by just looking at a half line, i.e., one edge only. Define

$$\phi_{j,k}^{\text{half}}(x) = \begin{cases} \phi_{j,k}(x) & \text{if } x \geq 0 \\ 0 & \text{if } x < 0 \end{cases}$$

$$V_j^{\text{half}} = \overline{\text{Span}\{\phi_{j,k}^{\text{half}};\, k \in \mathbb{Z}\}}.$$

The space V_j^{half} can also be viewed as the space of all restrictions to $[0, \infty)$ of functions in V_j. Suppose that both ϕ and ψ have been shifted so that support ϕ = support $\psi = [-N + 1, N]$. (We work with the N-vanishing moment family (1.7).) Then the $\phi_{j,k}^{\text{half}}$ with $k \leq -N$ vanish identically, and the $\phi_{j,k}^{\text{half}}$ with $k \geq N - 1$ are untouched. One can similarly define $\psi_{j,k}^{\text{half}}$; again, these are non-trivially affected by the restriction only if $-N < k < N - 1$. In Meyer [21] it is established (simpler proofs were subsequently given in Lemarié and Malgouyres [15]) that

1. The $\phi_{j,k}^{\text{half}}$, $-N + 1 \leq k \leq N - 2$, are all independent, and orthogonal to the "interior" $\phi_{j,m}^{\text{half}}$ with $m \geq N - 1$. Introducing the natural definition $W_j^{\text{half}} = V_{j-1}^{\text{half}} \cap (V_j^{\text{half}})^{\perp}$, one finds that
2. The interior $\psi_{j,k}^{\text{half}}$ (i.e., $k \geq N - 1$) are all in W_j^{half}.
3. However, the $\psi_{j,k}^{\text{half}}$ with $k = -N + 1, \ldots, -1$ are in V_j^{half}; i.e., $\text{Proj}_{W_j^{\text{half}}} \psi_{j,k}^{\text{half}} = 0$ for $-N + 1 \leq k \leq -1$.
4. On the other hand, the $\text{Proj}_{W_j^{\text{half}}} \psi_{j,k}^{\text{half}}$ with $0 \leq k \leq N - 2$ are non-vanishing, independent, and orthogonal to the interior $\psi_{j,m}^{\text{half}}$ with $m \geq N - 1$.

These facts can be exploited to construct an orthonormal wavelet basis adapted to the half line and the associated subband filtering scheme; the construction uses the following steps:

a. Orthonormalize the $\phi_{0,k}^{\text{half}}$, $-N + 1 \leq k \leq N - 2$; we call the resulting functions $\phi_{0,k}^{\text{edge}}$. Note that these are $2N - 2$ different functions; even though $\phi_{0,k}^{\text{half}}(x) = \phi_{0,N-1}^{\text{half}}(x - k + N - 1)$ if $k \geq N - 1$ and $x \geq 0$, no such thing is true for the orthonormal $\phi_{0,k}^{\text{edge}}$. We have

$$\phi_{0,k}^{\text{edge}} = \sum_{l=-N+1}^{N-2} A_{k,l} \phi_{0,l}^{\text{half}}, \tag{3.1}$$

where A is an invertible $(2N - 2) \times (2N - 2)$ matrix.

b. Since $\phi_{0,k}^{\text{half}} = \Sigma_m\, h_m \phi_{-1,2k+m}^{\text{half}}$, for all $k \geq -N + 1$, it follows that

$$\phi_{0,k}^{\text{edge}} = \sum_{l=-N+1}^{N-2} H_{k,l}^{\text{edge}} \phi_{-1,l}^{\text{edge}} + \sum_{m \geq N-1} h_{k,m}^{\text{edge}} \phi_{-1,m}^{\text{half}} \tag{3.2}$$

with

$$H_{k,l}^{\text{edge}} = \sum_{r=-N+1}^{N-2} \sum_{m=-N+1-2k}^{-2k+N-2} A_{k,r} h_m (A^{-1})_{2k+m,l},$$

$$h_{k,m}^{\text{edge}} = \sum_{r=-N+1}^{N-2} A_{k,r} h_{m-2r},$$

and the implicit assumption that $h_m = 0$ for $m < -N + 1$ or $m > N$. For the $\phi_{0,k}^{\text{half}}$, $k \geq N - 1$, the recursion is the same as it was on the whole line.

c. Compute, for $0 \leq k \leq N - 2$,

$$\tilde{\psi}_{0,k}^{\text{half}} = \text{Proj}_{W_0^{\text{half}}} \psi_{0,k}^{\text{half}} = \psi_{0,k}^{\text{half}} - \sum_{l=-N+1}^{N-2} \langle \psi_{0,k}^{\text{half}}, \phi_{0,l}^{\text{edge}} \rangle \phi_{0,l}^{\text{edge}},$$

and orthonormalize the results to obtain

$$\psi_{0,k}^{\text{edge}} = \sum_{l=0}^{N-2} B_{k,l} \psi_{0,l}^{\text{half}} + \sum_{l=-N+1}^{N-2} C_{k,l} \phi_{0,l}^{\text{edge}}.$$

d. From $\psi_{0,k}^{\text{half}} = \Sigma_m\, g_m \phi_{-1,2k+m}^{\text{half}}$ one then computes

$$\psi_{0,k}^{\text{edge}} = \sum_{l=-N+1}^{N-2} G_{k,l}^{\text{edge}} \phi_{-1,l}^{\text{edge}} + \sum_{m \geq N-1} g_{k,m}^{\text{edge}} \phi_{-1,m}^{\text{half}}, \tag{3.3}$$

with

$$G_{k,l}^{\text{edge}} = \sum_{r=0}^{N-2} \sum_{m=-N+1-2k}^{N-2k-2} B_{k,r} g_m (A^{-1})_{2k+m,l} + \sum_{s=-N+1}^{N-2} C_{k,s} H_{s,l}^{\text{edge}}$$

and

$$g_{k,m}^{\text{edge}} = \sum_{r=0}^{N-2} B_{k,r} g_{m-2r} + \sum_{s=-N+1}^{N-2} C_{k,s} h_{k,m}^{\text{edge}},$$

where we have again $g_n = 0$ for $n < 0$ or $n > 2N - 1$.

The filter coefficients can then be used in a multiresolution cascade, as usual. More precisely, the whole construction is invariant for dilation of x by 2^j, and (3.2), (3.3) are valid if $0, -1$ are replaced by $j, j - 1$.

The only steps in this program which are not completely explicit are the two orthonormalization steps. These can be done by a Gram–Schmidt procedure. If the Gram–Schmidt procedure for the edge scaling functions starts with $\phi_{0,-N+1}^{\text{half}}$, and moves on to larger values of k, so that $A_{k,l}$ is an

upper triangular matrix, then the low pass filter coefficients at the edge will still look "staggered"; i.e.,

$$H_{k,l}^{\text{edge}} = 0 \quad \text{if} \quad l > 2k + N,$$
$$h_{k,m}^{\text{edge}} = 0 \quad \text{if} \quad m > 2k + N,$$

as illustrated in Fig. 3. This results in "staggered" $\phi_{0,k}^{\text{edge}}$, i.e., support $\phi_{0,k}^{\text{edge}} = [0, N + k]$. One can of course also choose to Gram–Schmidt orthonormalize the vectors in a different order, leading to other (non-staggered) filter coefficients at the edge. Regardless of the procedure followed, we need the overlap matrix, i.e., the inner products $\langle \phi_{0,k}^{\text{half}}, \phi_{0,l}^{\text{half}} \rangle$, $-N + 1 \leq k, l \leq N - 2$, in order to compute the orthonormalization matrix A. These inner products can be computed explicitly, even though we do not have an analytic expression for ϕ. Because $\phi(x) = \sqrt{2}\, \Sigma_{n=-N+1}^{N} h_n \phi(2x - n)$, we have

$$\langle \phi_{0,k}^{\text{half}}, \phi_{0,l}^{\text{half}} \rangle = \int_0^\infty dx\, \phi(x - k)\overline{\phi(x - l)}$$
$$= \sum_{m,n} h_m \overline{h_n} \int_0^\infty dy \phi(y - 2k - m) \times \overline{\phi(y - 2l - n)}.$$

It follows that the $\lambda_{k,l} = \langle \phi_{0,k}^{\text{half}}, \phi_{0,l}^{\text{half}} \rangle$ satisfy

$$\lambda_{k,l} = \sum_{m,n=-N+1}^{N-2} h_m \overline{h_n} \lambda_{2k+m,2l+n}, \qquad -N + 1 \leq k, \quad l \leq N - 2. \quad (3.4)$$

If one takes into account that $\lambda_{r,s} = 0$ if r or $s \leq -N$, and $\lambda_{r,s} = \delta_{r,s}$ if r or $s \geq N - 1$, then (3.4) becomes a non-homogeneous linear system of $(N - 1)(2N - 3)$ equations for as many unknowns ($\lambda_{k,l} = \lambda_{l,k}$ because ϕ is real). This determines the overlap matrix of the $\phi_{0,k}^{\text{half}}$, so that step (a) can be carried out. In step (c) we need first the $\langle \psi_{0,k}^{\text{half}}, \phi_{0,l}^{\text{edge}} \rangle$ and then in addition the $\langle \psi_{0,k}^{\text{half}}, \psi_{0,l}^{\text{half}} \rangle$ in order to carry out the orthonormalization. Using $\psi_{0,k}^{\text{half}} = \Sigma_m g_m \phi_{-1,2k+m}^{\text{half}}$ and (3.1) together with (3.2), we can reduce those inner products to expressions involving only the filter coefficients, the matrix A, and the $\langle \phi_{-1,r}^{\text{half}}, \phi_{-1,s}^{\text{half}} \rangle = \lambda_{r,s}$ which we already know, so that step (c) too can be carried out without problems.

All this shows how Meyer's construction can be translated into an implementable scheme. On the interval, we have two edges to take into account, so that we have to find adapted scaling functions and wavelets for the boundary at 1 as well; they correspond to exactly the same computations, starting from h_n, g_n listed in the reverse order. We distinguish the two families by replacing the superscript "edge" by "left" for a left edge (corresponding to the half line $[0, \infty)$) and "right" for a right edge (corresponding to $(-\infty, 0]$). With out assumption that support ϕ = support $\psi = [-N + 1, N]$, the "interior" functions on the half line $(-\infty, 0]$ are the $\phi_{0,-l}$, $\psi_{0,-l}$ with $l \leq -N$, and the right edge functions are therefore labelled with $l \geq -N + 1$.

At sufficiently coarse scales, the two edges start to interact, in the sense that there are no "interior" scaling functions or wavelets, and all of them touch both 0 and 1. In that case one needs different definitions of the adapted scaling functions and wavelets (see Meyer [21]), leading to different filter coefficients. We do not go into these here; we assume that we never reach coarser approximation levels than j_0, where j_0 is the smallest integer such that $2^{j_0 - 1} \geq N$.

We have carried out these computations for $N = 2, 3, \ldots, 10$, starting from the wavelets and scaling functions with support width $[-N + 1, N]$, constructed in Daubechies [9], as well as for the less asymmetric variations from Daubechies [11]. In Tables 1 and 2 we list the adapted edge coefficients for the least asymmetric case, for $N = 2$ and 4, for both high and low pass filters. Tables for higher values of N can be obtained electronically; see the note at the end of the paper. Figures 4 and 5 show what the edge scaling functions and wavelets look like, in the cases $N = 2$ and 4, both at the left and at the right edge. The functions plotted are at resolution 0; i.e., they are in V_0^{half}, W_0^{half}, where the half line is $[0, \infty)$ for the left edge case, $(-\infty, 0]$ for the right edge. Note that not only the scaling functions, but also the wavelets are "staggered"; the $N - 1$ wavelets at the left edge, e.g., have supports $[0, 2N - 2], [0, 2N - 3], \ldots, [0, N]$, respectively. To achieve this, one needs an extra intermediate computation in step (c) above. First, observe that the $\psi_{0,k}^{\text{half}}$, $\phi_{0,k}^{\text{half}}$ with $k \leq N - 2$ all are linear combinations of the $\phi_{-1,l}^{\text{half}}$ with $l \leq 3N - 4$; it follows that the $\tilde{\psi}_{0,k}^{\text{half}}$ are as well. On the other hand, the $\tilde{\psi}_{0,-k}^{\text{half}}$ are all orthogonal to $\phi_{0,2N-3}^{\text{half}}$, which is a linear combination of the $\phi_{-1,k}^{\text{half}}$ with $3N - 5 \leq k \leq 5N - 3$. It follows that

$$0 = \sum_{m=0}^{1} \langle \tilde{\psi}_{0,k}^{\text{half}}, \phi_{-1,3N-5+m}^{\text{half}} \rangle \langle \phi_{-1,3N-5+m}, \phi_{0,2N-3} \rangle$$
$$= h_{-N+1} \langle \tilde{\psi}_{0,k}^{\text{half}}, \phi_{-1,3N-5}^{\text{half}} \rangle + h_{-N+2} \langle \tilde{\psi}_{0,k}^{\text{half}}, \phi_{-1,3N-4}^{\text{half}} \rangle,$$

for all $k = 0, \ldots, N - 2$. If we replace the $\tilde{\psi}_{0,k}^{\text{half}}$, $k = 0, \ldots, N - 3$, by $\tilde{\psi}_{0,k}^{\text{half}} - \langle \tilde{\psi}_{0,k}^{\text{half}}, \phi_{-1,3N-5} \rangle [\langle \tilde{\psi}_{0,N-2}^{\text{half}}, \phi_{-1,3N-5} \rangle]^{-1} \times \tilde{\psi}_{0,N-2}^{\text{half}}$, leaving $\tilde{\psi}_{0,N-2}^{\text{half}}$ untouched, then it follows that we have obtained a new (equivalent) family, all but one of which are linear combinations of the $\phi_{-1,l}^{\text{half}}$ with $l \leq 3N - 4$, and therefore supported in $[0, 2N - 3]$. We can repeat this trick, and end up with a family $\tilde{\psi}_{0,k}^{\text{half}}$, $k = 0, \ldots, N - 2$, each supported in $[0, N + k]$. These can then be orthonormalized, starting with the left-most one (i.e. $k = 1$), so that the staggered supports are preserved in the $\psi_{0,k}^{\text{edge}}$.

Several techniques can be used to plot the $\phi^{\text{edge}}, \psi^{\text{edge}}$ functions. One possibility is to keep track of all the basis trans-

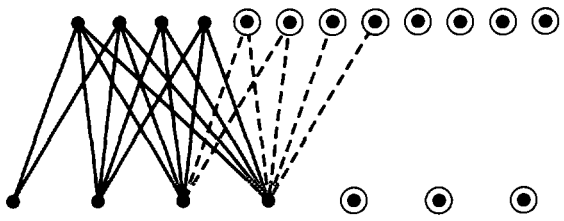

FIG. 3. Schematic representation of the non-zero $H_{k,l}^{\text{edge}}$ (solid lines), $h_{k,m}^{\text{edge}}$ (dashed lines) for $k = -2, -1, 0, 1$ in the case $N = 3$. The circled dots represent "interior" scaling functions; there are four edge scaling functions. Note that for $k = 1$ there are more than six non-zero filter coefficients; for general k, N there are $2(N + k)$ non-zero filter coefficients. We have assumed here that the Gram–Schmidt procedure starts from the leftmost $\phi_{0,k}^{\text{half}}$, and then works inward.

formations, and to plot simply the appropriate linear combinations of the $\phi_{-1,l}^{\text{half}}$, which can be plotted by any of the available techniques (using the refinement equation in a "cascade" algorithm, as in Daubechies [9] or Daubechies [10], using ergodicity of an associated flow, as in Berger [3], or using subdivision starting from the best initial conditions, as in Daubechies and Lagarias [12]). One can also use the cascade algorithm directly, with the adapted edge coefficients, to compute the $2^{J/2}\langle \phi_{0,k}^{\text{edge}}, \phi_{-J,l}\rangle$, $l \geq N - 1$, which tend to $\phi_{0,k}^{\text{edge}}(2^{-J}l)$ as J becomes large. This is how the graphs in Figs. 4 and 5 were plotted.

After this explanation of the construction and the computation of the filter or mask coefficients that would be used in the implementation of these bases in applications, we turn to a discussion of advantages and disadvantages.

The major advantage of the Meyer construction, indeed the main motivation for the construction, is that the resulting wavelet bases are unconditional bases for the Hölder spaces C^s. More precisely, if $\psi \in C^r$, then

$$\{\phi_{0,k}^{\text{half}}, \psi_{j,k}^{\text{half}}; j \leq 0, k \geq N - 1\}$$
$$\cup \{\phi_{0,k}^{\text{edge}}; k = -N + 1, \ldots, N - 2\}$$
$$\cup \{\psi_{j,k}^{\text{edge}}; j \leq 0, k = 0, \ldots, N - 2\}$$

is an unconditional basis for $C^s([0, \infty))$ if $s < r$ (with the understanding that for integer s Zygmund-class spaces have to be used). On the interval, we have that

$$\{\phi_{-j_0,k}; N - 1 \leq k \leq 2^{j_0} - N\}$$
$$\cup \{\psi_{-j,k}; j \geq j_0, N - 1 \leq k \leq 2^j - N\}$$
$$\cup \{\psi^0_{-j,k}; j \geq j_0, k = 0, \ldots, N - 2\}$$
$$\cup \{\psi^1_{-j,k}; j \geq j_0, k = 2^j - N + 1, \ldots, 2^j - 1\}$$

is an unconditional basis for $C^s([0, 1])$, where j_0 satisfies $2^{j_0 - 1} \geq N$ and where we define

$$\psi^0_{-j,k}(x) = 2^{j/2}\psi_{0,k}^{\text{left}}(2^j x)$$
$$\psi^1_{-j,2^j-l}(x) = 2^{j/2}\psi_{0,-l}^{\text{right}}(2^j(x - 1)).$$

These statements are proved in Meyer [21] (borrowing arguments from Meyer [20]). Basically, all that is needed is a generalization of the proof of Proposition 2.1 to larger values of s. The first step goes through if the wavelets are orthogonal to polynomials of degree at least $\lfloor s \rfloor$, the second step if all the wavelets and scaling functions used (including those at the edges) are in C^r with $r > s$. Both are easy to establish here, as follows. Let us restrict to the half line (the interval is analogous). Since polynomials up to degree $N - 1$ can be written as linear combinations of the $\phi_{0,k}$ on the whole line, the same is true on the half line, using the $\phi_{0,k}^{\text{half}}$, $k \geq -2N + 2$. By construction, the $\psi_{-j,k}^{\text{half}}$, j, $k \geq N - 1$ and the $\psi_{-j,k}^{\text{edge}}$, $j \geq 0$, $k = 0, \ldots, N - 2$ are orthogonal to those restricted scaling functions, so that they are orthogonal to all polynomials of degree $N - 1$ on $[0, \infty)$, and $N - 1 \geq r \geq \lfloor s \rfloor$. The second step is automatic: all the edge functions we have introduced are finite linear combinations of C^r-functions.

Are there disadvantages of the Meyer construction? There are several, more or less serious. One (minor) disadvantage is that we introduced $2N - 2$ scaling functions, but only $N - 1$ wavelets at each edge. This results in $\dim W_j^{[0,2]} = 2^j$, $\dim V_j^{[0,1]} = 2^j + 2N - 2$; the inequality of these dimensions

TABLE 1

The Filter Coefficients $H_{k,l}^{\text{edge}}$, $h_{k,l}^{\text{edge}}$ and $G_{k,l}^{\text{edge}}$, $g_{k,l}^{\text{edge}}$ (as in (3.2), (3.3)) for the Case $N = 2$, for Left and Right Edges, for Meyer's Construction

	l	$H_{k,l}$ or $h_{k,l}$	$G_{k,l}$ or $g_{k,l}$
		Left side	
$k = -1$	-1	0.848528137424	
	0	−0.529150262213	
$k = 0$	-1	0.132287565553	−0.512347538298
	0	0.212132034356	−0.821583836258
	1	0.838525491562	0.216506350947
	2	−0.484122918276	−0.125
		Right side	
$k = -1$	-3	0.484122918276	0.125
	-2	0.838525491562	0.216506350946
	-1	0.212132034356	−0.821583836258
	0	−0.132287565553	0.512347538298
$k = 0$	-1	0.529150262213	
	0	0.848528137424	

Note. In every case, the coefficients are listed from left to right ("outermost" coefficients first for the left side, last for the right side). The "interior" h_k are given by $h_{-1} = (1 + \sqrt{3})/4\sqrt{2}$, $h_0 = (3 + \sqrt{3})/4\sqrt{2}$, $h_1 = (3 - \sqrt{3})/4\sqrt{2}$, $h_2 = (1 - \sqrt{3})/4\sqrt{2}$.

TABLE 2
The Filter Coefficients $H_{k,l}^{\text{edge}}$, $h_{k,l}^{\text{edge}}$ and $G_{k,l}^{\text{edge}}$ $g_{k,l}^{\text{edge}}$ (as in (3.2), (3.3)) for the Case $N = 4$, for Left and Right Edges, for Meyer's Construction

	l	$H_{k,l}$ or $h_{k,l}$	$G_{k,l}$ or $g_{k,l}$
		Left side	
$k = -3$	−3	0.7983434920E + 00	
	−2	0.6022023488E + 00	
$k = -2$	−3	−0.3918024327E − 01	
	−2	0.5194149822E − 01	
	−1	−0.4817281609E + 00	
	0	0.8739021503E + 00	
$k = -1$	−3	0.1774707150E − 01	
	−2	−0.2352740580E − 01	
	−1	−0.1232594861E + 00	
	0	−0.6575127688E − 01	
	1	−0.9620570014E − 01	
	2	0.9850684416E + 00	
$k = 0$	−3	−0.2636405192E − 01	0.5979027428E + 00
	−2	0.3495099166E − 01	−0.7926434769E + 00
	−1	0.8114147375E + 00	−0.1659403671E − 01
	0	0.4440233637E + 00	0.6477069526E − 01
	1	0.3192581817E + 00	0.9713044594E − 01
	2	0.1636579832E + 00	−0.1797030610E − 01
	3	−0.4282797155E − 01	−0.3192898087E − 03
	4	0.1094933054E + 00	0.8162911886E − 03
$k = 1$	−3	−0.1670338745E − 01	0.4823971249E − 01
	−2	0.2214378721E − 01	−0.6395169431E − 01
	−1	−0.1643714751E − 01	0.3010034664E + 00
	0	−0.1112580065E − 01	0.1718883936E + 00
	1	0.2995602574E + 00	−0.8873256413E + 00
	2	0.2728668922E − 01	−0.3991915695E − 01
	3	0.8472064764E + 00	0.2462565991E + 00
	4	−0.4270166998E + 00	−0.1524149055E + 00
	5	−0.3309408518E − 01	−0.9080945357E − 02
	6	0.8460780753E − 01	0.2321619929E − 01
$k = 2$	−3	0.2727915769E − 02	−0.1162436086E − 02
	−2	−0.3616415322E − 02	0.1541048928E − 02
	−1	−0.5206157868E − 01	0.2218479707E − 01
	0	−0.2836107693E − 01	0.1208539488E − 01
	1	−0.4413123462E − 01	0.1880547055E − 01
	2	−0.1285294872E − 01	0.5476976811E − 02
	3	0.4543141690E + 00	−0.8114432093E − 01
	4	0.8282235028E + 00	−0.3089428579E + 00
	5	0.3000539798E + 00	0.8028339176E + 00
	6	−0.1037443976E + 00	−0.4957693566E + 00
	7	−0.1262470890E − 01	−0.2962669767E − 01
	8	0.3227612835E − 01	0.7574314021E − 01

	l	$H_{k,l}$ or $h_{k,l}$	$G_{k,l}$ or $g_{k,l}$
		Right side	
$k = -3$	−9	−.7576592267E − 01	−.3222260624E − 01
	−8	−.2963561006E − 01	−.1260377467E − 01
	−7	.4975940883E + 00	.9927560389E − 01
	−6	.8037308455E + 00	.2978757620E + 00
	−5	.2979273796E + 00	−.8039165735E + 00
	−4	−.9898430109E − 01	.4970737994E + 00
	−3	−.1322822645E − 01	.3110390157E − 01
	−2	.3237561509E − 01	−.7612569630E − 01
	−1	−.1031248132E − 02	.2424802864E − 02
	0	−.3127686214E − 02	.7354216650E − 02
	1	.1791458461E − 02	−.4212306812E − 02
	2	.1517778961E − 02	−.3568796441E − 02
$k = -2$	−7	−.7658857852E − 01	−.3043501638E − 01
	−6	−.2995738760E − 01	−.1190456375E − 01
	−5	.4965300858E + 00	.9317065775E − 01
	−4	.8099281192E + 00	.2811169922E + 00
	−3	.2555397153E + 00	−.7578721046E + 00
	−2	−.6529437751E − 01	.4453190863E + 00
	−1	.7039069384E − 01	−.1860863715E + 00
	0	.7744666189E − 01	−.2220387757E + 00
	1	.7703595608E − 01	−.1783088893E + 00
	2	.6526723504E − 01	−.1510687917E + 00
$k = -1$	−5	−.9324840456E − 01	−.1463677268E − 02
	−4	−.3647382930E − 01	−.5725128576E − 03
	−3	.2929411530E + 00	.6432723254E − 02
	−2	.8548427224E + 00	.1377492249E + 00
	−1	.1612498760E + 00	.2189246565E + 00
	0	.1056438759E + 00	.7323866487E + 00
	1	.2816233337E + 00	−.4805345237E + 00
	2	.2385999858E + 00	−.4071236849E + 00
$k = 0$	−3	−.5228106380E + 00	
	−2	−.2021221071E + 00	
	−1	.3973740339E + 00	
	0	.4284467101E + 00	
	1	.4477229118E + 00	
	2	.3793246746E + 00	
$k = 1$	−1	−.8535656929E + 00	
	0	.4620817304E + 00	
	1	.1836012602E + 00	
	2	.1555526555E + 00	
$k = 2$	1	−.6464210153E + 00	
	2	.7629809380E + 00	

Note. In every case, the coefficients are listed from left to right ("outermost" coefficients first for the left side, last for the right side). In this case the "interior" h_n are

$$h_{-3} = -.07576571478950, \quad h_{-2} = -.02963552764600, \quad h_{-1} = .4976186676328,$$
$$h_0 = .8037387518051, \quad h_1 = .29785779560531, \quad h_2 = -.0992195435766,$$
$$h_3 = -.01260396726203, \quad h_4 = .03222310060405.$$

means that the adapted filters cannot be used for wavelet packet constructions on $[0, 1]$.

There is a second, more serious disadvantage, stemming from the nature of the construction itself, more precisely from the definition of the $\phi_{0,k}^{\text{half}}$ as restrictions of ϕ. For reasonably large values of N ($N \geq 5$ in practice), ϕ is smooth and mostly concentrated on a fraction of its support $[-N + 1, N]$, so that $\|\phi_{0,N-2}^{\text{half}}\|^2$ is very close to 1, and $\|\phi_{0,-N+1}^{\text{half}}\|^2$ is very small. One consequence is that the overlap matrix $\langle \phi_{0,k}^{\text{half}}, \phi_{0,l}^{\text{half}} \rangle$ tends to be very ill conditioned

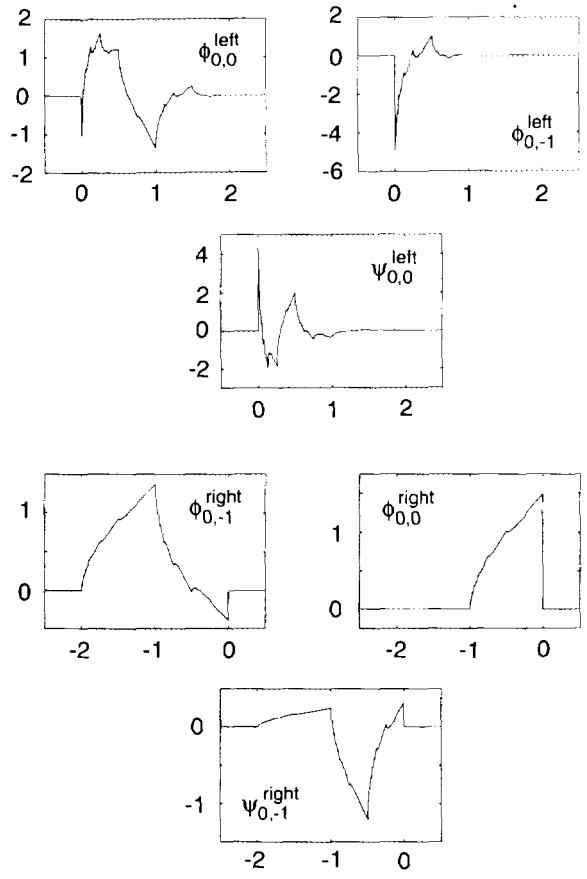

FIG. 4. The orthonormal scaling functions and wavelets for $N = 2$ in Meyer's construction, at a left edge (i.e., on $[0, \infty)$) or a right edge (on $(-\infty, 0]$). Note that the scaling functions have "staggered" supports. The indexing convention is explained in the text.

when N is large. The following trivial computation makes this more quantitative:

$$\int_0^\infty dx|\phi(x+N-1)|^2$$
$$= \sum_{m,n=-N+1}^{N} 2h_m\overline{h_m}\int_0^1 dx\phi(2x+2N-2-n)$$
$$\times \phi(2x+2N-2-m)$$
$$\leqslant |h_N|^2\int_0^1 dy|\phi(y+N-2)|^2$$
$$+ |h_{N-1}|^2\int_0^1 dy|\phi(y+N-1)|^2$$
$$+ 2|h_N||h_{N-1}|\int_0^2 dy|\phi(y+N-2)||\phi(y+N-1)|;$$

using $\int_0^1 dy|\phi(y+N-2)|^2 \leqslant \|\phi\|^2 = 1$ (a very coarse bound), this leads to

$$\int_0^\infty dx|\phi(x+N-1)|^2 \leqslant \frac{|h_N|^2 + |h_{N-1}||h_N|}{1 - |h_N|^2 - |h_{N-1}|^2 - |h_{N-1}||h_N|},$$

provided the denominator in the right hand side is positive. A similar bound, with h_{-N+1}, h_{-N+2} replacing h_N, h_{N-1}, respectively, holds for $\int_{-N+1}^{-N+2} dx|\phi(x)|^2$, so that

$$\int_0^\infty dx|\phi(x-N+2)|^2$$
$$= 1 - \int_{-N+1}^{-N+2} dx|\phi(x)|^2$$
$$\geqslant \frac{1 - |h_{-N+2}|^2}{1 - |h_{-N+1}|^2 - |h_{-N+2}|^2 - |h_{-N+1}||h_{-N+2}|}.$$

It follows that the condition number of the overlap matrix, i.e.,

$$\Big[\sup_{\Sigma_k|\lambda_k|^2=1}\sum_{k,l=-N+1}^{N-2}\lambda_k\overline{\lambda_l}\langle\phi^{half}_{0,k},\phi^{half}_{0,l}\rangle\Big]$$
$$\times\Big[\lim_{\Sigma_k|\mu_k|^2=1}\sum_{k,l=-N+1}^{N-2}\mu_k\overline{\mu_l}\langle\phi^{half}_{0,k},\phi^{half}_{0,l}\rangle\Big]^{-1}, \quad (3.5)$$

is bounded below by

$$[1 - |h_{-N+2}|^2][1 - |h_N|^2 - |h_{N-1}|^2 - |h_N||h_{N-1}|]$$
$$\times[1 - |h_{-N+1}|^2 - |h_{-N+2}|^2 - |h_{-N+1}||h_{-N+2}|]^{-1}$$
$$\times[|h_N|^2 + |h_{N-1}||h_N|]^{-1}. \quad (3.6)$$

For $N = 4$, (3.6) is of the order of 10^3, but its value increases rapidly with N; for $N = 10$, it is $\sim 4 \times 10^7$. Since (3.6) is only a very coarse lower bound for (3.5), the true conditioning number is in fact even larger. This ill conditioning makes the computation of the adapted filter coefficients near the edges rather tricky; for N larger than 6, for instance, we already needed quadruple precision. The computation of the overlap matrix itself, along the lines outlined before, is quite tricky itself as well, involving the inversion of a large badly conditioned matrix.

The disequilibrium between $\|\phi^{half}_{0,N-2}\|^2$ and $\|\phi^{half}_{0,-N+1}\|^2$ also expresses itself in other ways. One application of wavelet bases and multiresolution on the interval is the "natural" extension of functions living on the interval to functions on the whole line. Since the edge-wavelets and scaling functions can all be written as linear combinations of restrictions of whole-line functions, one can extend them trivially by "gluing their tails on again," i.e., by replacing every $\phi^{half}_{-j,k}$

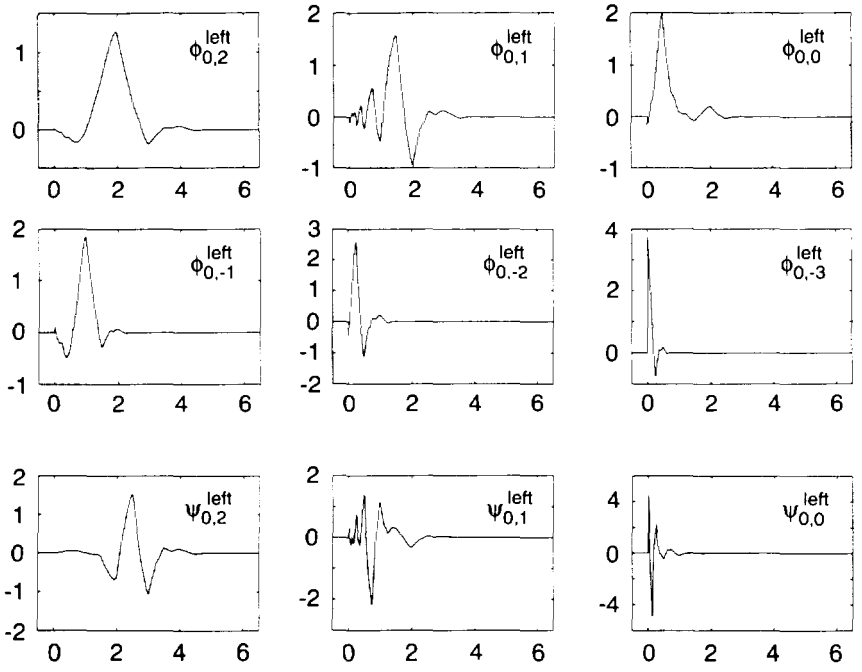

FIG. 5a. The orthonormal scaling functions and wavelets for $N = 4$ in Meyer's construction on the half line $[0, \infty)$. Note that the six scaling functions ϕ_k^{left} and the three wavelets ψ_k^{left} have supports $[0, 4 + k]$.

by $\phi_{-j,k}$. If this is done for every edge term in the expansion of a function f on $[0, \infty)$, the result is a smooth function f^{ext} extending f to $\mathbb{R}$, with the appealing property that the high frequency components in f spread out less to $(-\infty, 0]$ than the low frequency components. At any scale j, the extension is limited to $[-2^{-j}(2N - 2), \infty)$. With the present construction this does not work so well in practice, however: because $\phi^{\text{edge}}_{0,-N+1} = \phi^{\text{half}}_{0,-N+1}/\|\phi^{\text{half}}_{0,-N+1}\|$, the extension of $\phi^{\text{edge}}_{0,-N+1}$ to the left half line has a huge amplitude, ranging up to $\max|\phi(x)|/\|\phi^{\text{half}}_{0,-N+1}\| \simeq \|\phi^{half}_{0,-N+1}\|^{-1}$. In fact, this is the reason Jawerth, in an application involving such extension operators for surface design in collaboration with Dahlberg, decided to develop a construction different from Meyer's.

A third instance where one can feel the imbalance among the $\phi^{\text{half}}_{0,k}$ is in the plots of the edge functions. Typically, $\phi^{\text{half}}_{0,-N+1}$ has much faster high amplitude oscillations than ϕ itself (the same oscillations are of course present in the tail of ϕ, but with exceedingly small amplitude); because of the orthonormalization procedure, this oscillatory behavior can typically spread to several edge scaling functions, as in Fig. 5. This is disturbing: we like to think of wavelets at a certain scale as corresponding to a frequency band of about one octave, and the edge wavelets in Figure 5, corresponding to just one scale, clearly cover may octaves.

In the next section we present a different construction that avoids all these problems, while still giving good bases for the C^r-spaces.

4. A DIFFERENT FAMILY OF ORTHONORMAL WAVELET BASES ON [0, 1]

Our starting point is again the N vanishing moment family (1.7); our goal is to adapt this family in such a way near the edges of the interval that we obtain unconditional bases for $C^s([0, 1])$. As emphasized already in Sections 2 and 3, this can be achieved by retaining the interior scaling functions, and adding adapted edge scaling functions in such a way that their union still generates all polynomials on $[0, 1]$, up to a certain degree. Our construction in this section results from taking this prescription literally. We start again by illustrating the construction on the half line $[0, \infty)$. The "interior" scaling functions at scale 0 are the $\phi_{0,k}$ with $k \geq N - 1$; they are supported on $[0, \infty)$. By themselves, the interior $\phi_{0,k}$ do not even generate the constants on $[0, \infty)$, as is clear from $\phi_{0,k}(0) = \phi(-k) = 0$ for all $k \geq N - 1$. Let us therefore add the constants "by hand." We define an edge function ϕ^0 by

$$\phi^0(x) = 1 - \sum_{k=N-1}^{\infty} \phi(x - k).$$

The interior $\phi_{0,k}$ and this edge function ϕ^0 together generate all the constants on $[0, \infty)$. Moreover, because

$$\sum_{k=-\infty}^{\infty} \phi(x - k) = 1,$$

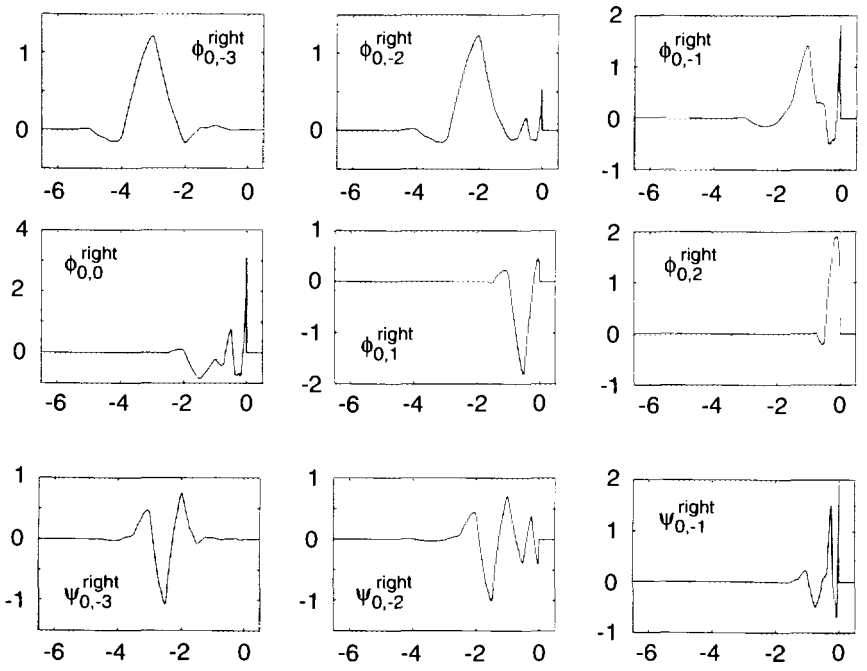

FIG. 5b. Same as Fig. 5a, but on the half line $(-\infty, 0]$.

we also have, for $0 \leq x < \infty$,

$$\phi^0(x) = \sum_{k=-\infty}^{N-2} \phi(x-k) = \sum_{k=-N+1}^{N-2} \phi(x-k),$$

showing that ϕ^0 has compact support. It also shows, incidentally, that ϕ^0 is orthogonal to all the interior $\phi_{0,k}$. The only thing that we have to check is that by adding functions in this ad hoc way we do not leave the framework of a multiresolution hierarchy. We have, however,

$$\phi(x-k) = \sqrt{2} \sum_{l=2k-N+1}^{N+2k} h_{l-2k}\phi(2x-l)$$

and

$$\phi^0(x) = \phi^0(2x) + \sum_{l=N-1}^{\infty} \phi(2x-l)[1 - \sqrt{2} \sum_{k=N-1}^{\infty} h_{l-2k}]$$

$$= \phi^0(2x) + \sum_{l=N-1}^{3N-4} \phi(2x-l)[1 - \sqrt{2} \sum_{k=\lceil (l-N)/2 \rceil}^{\lfloor (l+N-1)/2 \rfloor} h_{l-2k}],$$

where we have used that $h_n = 0$ for $n < -N+1$ or $n > N$ and $\Sigma_n h_{2n} = 1/\sqrt{2} = \Sigma_n h_{2n+1}$. It follows therefore that

$$\text{Span}\{\phi^0, \phi_{0,k}; k \geq N-1\} \subset \text{Span}\{\phi^0(2\cdot), \phi_{-1,k}; k \geq N-1\}.$$

Similar inclusions hold immediately if we scale by other integer powers of 2, and we still have a hierarchy of nested spaces.

This is essentially all there is to the construction we propose here. If we want the edge + interior scaling functions to generate more polynomials than only the constants, then we have to add in, by hand, more edge functions (for the polynomials up to degree L, we add in total $L+1$ functions). If we work on the interval, then the same has to be done at the other edge as well. On the other hand, as pointed out earlier, for many applications it is desirable to have exactly 2^j scaling functions of scale j when working on $[0, 1]$. Let us count how much room this leaves us for adding extra functions at the edges. If we start from a minimal support N-vanishing moment wavelet, then support $\phi = [-N+1, N]$, and for j sufficiently large we have exactly $2^j - 2N + 2$ interior scaling functions at scale j. This leaves room for adding $N-1$ ad hoc functions at each edge, so that the total family can generate polynomials of degree at most $N-2$. The unaltered whole-line scaling functions can generate all polynomials up to degree $N-1$ (see Section 1), so that we seem to have "lost" one degree. In order to recover this one extra degree (and so be able to characterize the $C^s([0, 1])$ spaces for the same range of s as we could on all of $\mathbb{R}$), we have to make room for one extra function at each edge of the interval. For this reason we abandon the two outermost interior scaling functions, which corresponds to retaining only the $\phi_{0,k}$ with $k \geq N$ rather than $k \geq N-1$ on the half line.

Let us now be more precise. For given N, we define the N edge functions $\tilde{\phi}^k$, $k = 0, \ldots, N-1$, on $[0, \infty)$ by

$$\tilde{\phi}^k(x) = \sum_{n=0}^{2N-2} \binom{n}{k} \phi(x + n - N + 1)$$
$$= \sum_{n=k}^{2N-2} \binom{n}{k} \phi(x + n - N + 1) \qquad (4.1)$$

These are all compactly supported, and their supports are staggered, i.e., support $\tilde{\phi}^k = [0, 2N - 1 - k]$. The following proposition summarizes some of their properties:

PROPOSITION 4.1. *The N functions $\tilde{\phi}^k$, $k = 0, \ldots, N-1$, are independent, and orthogonal to the $\phi_{0,m}$, $m \geq N$. Together with the $\phi_{0,m}$, $m \geq N$, they generate all the polynomials up to degree $N-1$ on $[0, \infty)$. Finally, there exist constants $a_{k,l}$, $b_{k,m}$ such that*

$$\tilde{\phi}^k(x) = \sum_{l=0}^{k} a_{k,l} \tilde{\phi}^l(2x) + \sum_{m=N}^{3N-2-2k} b_{k,m} \phi(2x - m). \qquad (4.2)$$

Proof.

1. The independence of the $\tilde{\phi}^k$ follows immediately from their staggered supports. Orthogonality with respect to the $\phi_{0,m}$, $m \geq N$, is also immediate from (4.1) and the orthonormality of the $\phi_{0,n}$, $n \in \mathbb{Z}$.

2. For every $k = 0, \ldots, N-1$, the function $(1/k!)y(y-1)\cdots(y-k+1)$ is a polynomial in y of degree k. It follows that these functions can be transformed by a simple (triangular) transformation into the polynomials $1, x, \ldots, x^{N-1}$. This is true in particular if $y = n$. Define now

$$\mathring{\phi}^k(x) = \sum_{n=0}^{2N-2} n^k \phi(x + n - N + 1),$$
$$k = 0, \ldots, N-1, \qquad (4.3)$$

with again $x \in [0, \infty)$. Then the $\tilde{\phi}^k$ and $\phi_{0,m}$, $m \geq N$ generate all the polynomials of degree up to $N-1$ if and only if the same holds for the $\mathring{\phi}^k$ and $\phi_{0,m}$, $m \geq N$.

3. We now establish some properties of the $\mathring{\phi}^k$. We start by noting that, for $k = 0, \ldots, N-1$,

$$\sum_{n \in \mathbb{Z}} (x - n)^k \phi(x - n) = C_k := \int_{-\infty}^{\infty} dx\, x^k \phi(x). \qquad (4.4)$$

To see this, note that the left hand side is a periodic function with period 1; it is therefore completely characterized by its Fourier coefficients, which are, up to a constant, equal to the derivatives $\hat{\phi}^{(k)}(2\pi l)$. Now

$$\hat{\phi}^{(k)}(2\pi l) = 2^{-k} \sum_{r=0}^{k} \binom{k}{r} m_0^{(r)}(\pi l) \hat{\phi}^{(k-r)}(\pi l).$$

If $l \neq 0$ is odd, then $m_0^{(r)}(\pi) = 0$ for $r = 0, \ldots, N-1$ insures that $\hat{\phi}^{(k)}(2\pi l) = 0$. This in turn, by applying the equation again, implies that $\hat{\phi}^{(k)}(2\pi l) = 0$ if $l \neq 0$ is even. Consequently the left hand side of (4.4) is constant; by integration from 0 to 1 one immediately establishes the rest of (4.4). Note that the C_l can be computed from the h_n in the following way,

$$C_l = \sqrt{2} \sum_m h_m \int dx\, x^l \phi(2x - m)$$
$$= 2^{-l-1/2} \sum_m h_m \int dy\, \phi(y)(y + m)^l$$
$$= 2^{-l} \sum_{r=0}^{l} \binom{l}{r} M_r C_{l-r},$$

with $M_r = 2^{-1/2} \sum_m h_m m^r$. In particular, $M_0 = 1$, so that

$$C_l = (2^l - 1)^{-1} \sum_{r=1}^{l} \binom{l}{r} M_r C_{l-r}.$$

4. As a consequence of (4.4) we have, for $k = 0, \ldots, N-1$,

$$\sum_{n \in \mathbb{Z}} n^k \phi(x - n - N + 1)$$
$$= \sum_n [x - N + 1 - (x - n)]^k \phi(x - n)$$
$$= \sum_{l=0}^{k} \binom{k}{l} (-1)^l (x - N + 1)^{k-l} C_l;$$

we denote these polynomials $p_k(x)$. They are of degree k and their leading order term is exactly x^k, since $C_0 = 1$. It follows that the N polynomials p_k are independent; together they generate all polynomials of degree up to $N-1$. From (4.3) we see that for $x \in [0, \infty)$

$$p_k(x) = (-1)^k \mathring{\phi}^k(x) + \sum_{n=1}^{\infty} n^k \phi(x - n - N + 1),$$

so that the $\mathring{\phi}^k$, together with the $\phi_{0,m}$, $m \geq N$, do indeed generate all the polynomials up to degree $N-1$.

5. It remains to establish the recurrence (4.2). Again, it is sufficient to prove a similar recurrence for the $\mathring{\phi}^k$. We have

$$\tilde{\phi}^k(x) = \sum_{n=0}^{2N-2} n^k \sum_{m=-N+1}^{N} \sqrt{2} h_m \phi(2x - 2N + 2 + 2n - m)$$

$$= \sqrt{2} \sum_{l=-N+1}^{N-1} \phi(2x - l) \sum_{n=0}^{2N-2} h_{2n-2N+2+l} n^k$$

$$+ \sqrt{2} \sum_{r=N}^{3N-2} \phi(2x - r) \sum_{n=-N+1}^{N-1} (n + N - 1)^k h_{2n+r}, \tag{4.5}$$

where we have used $x \geq 0$, and we implicitly assume, as always, that $h_m = 0$ for $m < -N + 1$ or $m > N$. The second term is already of the right form (the range on r is more limited in (4.2) because of the staggered supports for the $\tilde{\phi}^k$, a property which the $\tilde{\tilde{\phi}}^k$ do not share); it remains to check that the first term can be recast into a linear combination of the $\tilde{\tilde{\phi}}^l(2x)$, $l = 0, \ldots, k$. Note first that we can lift the restriction on n in this sum: for $n < 0$ or $n > 2N - 2$ the $h_{2n-2N+2+l} \equiv 0$ if $-N + 1 \leq l \leq N - 1$. Next note that

$$\sqrt{2} \sum_n h_{2n-2N+2+l} n^k$$

$$= 2^{-k+1/2} \sum_n h_{2n-N+1-(N-l-1)} (2n)^k$$

$$= 2^{-k+1/2} \sum_{r=0}^{k} \binom{k}{r} (N - l - 1)^r$$

$$\times \sum_n h_{2n-N+1-(N-l-1)} [2n - (N - l - 1)]^{k-r}$$

$$= 2^{-k+1/2} \sum_{r=0}^{k} \binom{k}{r} (N - l - 1)^r \mu_{N-1,k-r}, \tag{4.6}$$

where we have used that $m_0^{(s)}(\pi) = 0$ for $s = 0, \ldots, N - 1$, which implies $\Sigma_n h_n (-1)^n n^s = 0$, hence

$$\sum_n h_{n-t} (-1)^n n^r = (-1)^t \sum_m h_m (-1)^m (m + t)^r$$

$$= (-1)^t \sum_{s=0}^{r} \binom{r}{s} t^{r-s} \sum_m h_m (-1)^m m^s = 0$$

for $r = 0, \ldots, N - 1$, so that

$$\sum_m h_{2m-t} (2m)^r = \mu_{t,r} = \sum_m h_{2m+1-t} (2m + 1)^r$$

$$= \frac{1}{2} \sum_n h_{n-t} n^r = \frac{1}{\sqrt{2}} \sum_{l=0}^{r} \binom{r}{l} t^l M_{r-l}.$$

Substituting (4.6) into (4.5) immediately leads to the desired recurrence. ▩

Remark. The only thing we have not spelled out in numerical detail is the transition from the polynomials $\binom{n}{k}$ to the n^k (and back again), but this triangular transformation is both well known and easy to derive (the entries of the triangular matrix satisfy easy recurrence relations). Otherwise everything in this construction is completely explicit. In particular, one easily checks that $a_{k,k} = 2^{-k}$.

Define now

$$V_{-j}^{\text{left}} = \overline{\text{Span}[\{\tilde{\phi}^k(2^j \cdot); k = 0, \ldots, N - 1\} \cup \{\phi_{-j,m}; m \geq N\}]}.$$

(The superscript "left" stands here for a half line with an endpoint and correspondingly adapted scaling functions at the left end.) Proposition 4.1 establishes that the V_{-j}^{left} constitute a multiresolution hierarchy,

$$\cdots \subset V_2^{\text{left}} \subset V_1^{\text{left}} \subset V_0^{\text{left}} \subset V_{-1}^{\text{left}} \subset V_{-2}^{\text{left}} \subset \cdots.$$

Since $\overline{\cup_j \text{Span}\{\phi_{-j,m}; m \geq N\}}$ already equals $L^2([0, \infty))$, we also immediately have $\overline{\cup_j V_j^{\text{left}}} = L^2([0, \infty))$. One can obtain an orthonormal basis for V_0^{left} by orthonormalizing the $\tilde{\phi}^k$, since they are already orthogonal to the orthonormal $\phi_{0,m}$; scaling them leads to an orthonormal basis for every V_j^{left}. If one orthonormalizes by a Gram–Schmidt procedure, starting with $\tilde{\phi}^{N-1}$, and working down to lower values of k, then the resulting orthonormal ϕ_k^{left}, $k = 0, \ldots, N - 1$, still have staggered supports: support $\phi_k^{\text{left}} = [0, N + k]$. (We have chosen this indexing because the ϕ_k^{left} replace, in a way, the $\phi_{0,l}$, $l \leq N - 1$. Consistent with the other notations, we denote by $\phi_{-j,k}^{\text{left}}(x)$ the functions $2^{j/2} \phi_k^{\text{left}}(2^j x)$.) To carry out the Gram–Schmidt orthonormalization explicitly, we need again the overlap matrix $\langle \tilde{\phi}^k, \tilde{\phi}^l \rangle$. To compute this overlap matrix, we use the recurrence (4.2). For $k = 0$, for instance, we have

$$\|\tilde{\phi}^0\|^2 = a_{0,0}^2 \frac{1}{2} \|\tilde{\phi}^0\|^2 + \sum_{m=N}^{3N-2} b_{0,m}^2 \frac{1}{2},$$

from which we obtain $\|\tilde{\phi}^0\|^2$. It then follows that

$$\langle \tilde{\phi}^0, \tilde{\phi}^1 \rangle = a_{0,0} a_{1,0} \frac{1}{2} \|\tilde{\phi}^0\|^2$$

$$+ a_{0,0} a_{1,1} \frac{1}{2} \langle \tilde{\phi}^0, \tilde{\phi}^1 \rangle + \frac{1}{2} \sum_{m=N}^{3N-4} b_{0,m} b_{1,m},$$

leading to an explicit formula for $\langle \tilde{\phi}^0, \tilde{\phi}^1 \rangle$, since $\|\tilde{\phi}^0\|^2$ is known. It is now clear how to proceed for higher values of k. If all the $\langle \tilde{\phi}^k, \tilde{\phi}^l \rangle$ for $0 \leq k, l \leq K - 1$ are known, then we can compute the $\langle \tilde{\phi}^k, \tilde{\phi}^K \rangle$ for $k = 0, \ldots, K$ in that order. We obtain equations of the type

$$[1 - \tfrac{1}{2}a_{k,k}a_{K,K}]\langle \tilde{\phi}^k, \tilde{\phi}^K \rangle$$

$$= \text{linear combination of the } \langle \tilde{\phi}^l, \tilde{\phi}^K \rangle \text{ with } l < k$$

$$\text{and of the } \langle \tilde{\phi}^l, \tilde{\phi}^m \rangle \text{ with } l, m \leq K + \text{constants.}$$

Since $\frac{1}{2}a_{k,k}a_{K,K} = 2^{-k-K-1} \leq \frac{1}{2}$, this immediately leads to a numerically stable recursive scheme for determining the $\langle \tilde{\phi}^k, \tilde{\phi}^l \rangle$. (Equivalently, we have to invert an $N(N+1)/2$ triangular system with a condition number bounded by 2, a distinct improvement over the situation in the previous section.)

The orthonormal ϕ_k^{left}, constructed with staggered supports along the lines indicated above, satisfy a recursion relation similar to (4.2) and inherited by all the scales j. Explicitly, there exist constants $H_{k,l}^{\text{left}}$ and $h_{k,m}^{\text{left}}$ (which can be computed explicitly from the $a_{k,l}$, $b_{k,l}$ in (4.2) and the orthonormalization procedure) such that

$$\phi_{-j,k}^{\text{left}} = \sum_{l=0}^{N-1} H_{k,l}^{\text{left}} \phi_{-j-1,l}^{\text{left}} + \sum_{m=N}^{N+2k} h_{k,m}^{\text{left}} \phi_{-j-1,m}. \tag{4.7}$$

All this was on the half line. If we work on the interval $[0, 1]$, and we start with a scale fine enough so that the two edges do not interact, i.e., $2^j \geq 2N$, then there are $2^j - 2N$ interior scaling functions $\phi_{-j,N}, \ldots, \phi_{-j,2^j-N-1}$, and we add N functions at each end. At 0, we have the functions defined above, $\phi_{-j,k}^0 = \phi_{-j,k}^{\text{left}}$, $k = 0, \ldots, N-1$. To obtain the extra functions at 1, we first have to repeat the construction above for the half line $(-\infty, 0]$ (or equivalently, repeat the construction on $[0, \infty)$ for the reflected coefficients $h_n^{\#} = h_{-n+1}$). This leads to functions $\phi_{-j,k}^{\text{right}}(x) = 2^{j/2}\phi_k^{\text{right}}(2^j x)$, $k = -1, -2, \ldots, -N$ with support $[k - N + 1, 0]$ (again the indexing has been chosen so that the k-values complement the interior functions $\phi_{-j,m}$, $m \leq -N-1$, where the outermost interior function has not been retained, as before. If everything is recast in terms of the #-construction, then $\phi_k^{\text{right}}(x) = \phi_{-1-k}^{\#,\text{left}}(-x)$.) On the interval, the adapted scaling functions at 1 are then given by $\phi_{-j,2^j-l}^1(x) = \phi_{-j,-l}^{\text{right}}(x-1)$, $l = 1, \ldots, N$. Together, the $\phi_{-j,k}^0$, $k = 0, \ldots, N-1$, $\phi_{-j,m}$, $m = N, \ldots, 2^j - N + 1$, and $\phi_{-j,r}^1$, $r = 2^j - N, \ldots, 2^j - 1$, constitute an orthonormal basis for the 2^j-dimensional space $V_j^{[0,1]}$.

We now turn to the wavelets rather than the scaling functions. As usual, we define $W_j^{[0,1]} = V_{j-1}^{[0,1]} \cap (V_j^{[0,1]})^{\perp}$. From dimension counting, it immediately follows that $\dim W_j^{[0,1]} = 2^j$. On the other hand it is easy to check that the $2^j - 2N$ functions $\psi_{-j,m}$, $m = N, \ldots, 2^j - N - 1$, are all in $W_j^{[0,1]}$. Since they are all orthonormal, we therefore need to add an extra $2N$ wavelets (N at each edge) to provide an orthonormal basis for $W_j^{[0,1]}$. We show here how to construct those at 0, the left end of the interval; the right end construction at 1 is of course analogous. To simplify notation, we return to the half line $[0, \infty)$. We define there $W_j^{\text{left}} = V_{j-1}^{\text{half}} \cap (V_j^{\text{half}})^{\perp}$; the $\psi_{j,m}$, $m \geq N$ all belong to W_j^{left}, and we are looking for N extra functions in W_j^{left}, orthonormal to these $\psi_{j,m}$. The following proposition tells us where to look:

PROPOSITION 4.2. *Define the functions* $\tilde{\psi}^k$, $k = 0, \ldots, N-1$, *by*

$$\tilde{\psi}^k = \phi_{-1,k}^{\text{left}} - \sum_{m=0}^{N-1} \langle \phi_{-1,k}^{\text{left}}, \phi_{0,m}^{\text{left}} \rangle \phi_{0,m}^{\text{left}}. \tag{4.8}$$

Then the $\tilde{\psi}^k$ *are* N *independent functions in* W_0^{left}, *orthogonal to the* $\psi_{0,m}$, $m \geq N$.

Proof.

1. The $\phi_{-1,k}^{\text{left}}$, $k = 0, \ldots, N-1$, are by construction orthogonal to the $\phi_{-1,m}$, $m \geq N$. Since the $\phi_{0,l}$, $\psi_{0,l}$ with $l \geq N$ are all linear combinations of the $\phi_{-1,m}$, $m \geq N+1$, it follows that $\phi_{-1,k}^{\text{left}} \perp \phi_{0,l}$, $\psi_{0,l}$ with $l \geq N$. Consequently $\tilde{\psi}^k$ is nothing but the orthonormal projection of $\phi_{-1,k}^{\text{left}}$ onto W_0^{left}. Moreover, as a linear combination of functions orthogonal to the $\psi_{0,m}$, $m \geq N$, $\tilde{\psi}^k$ is obviously orthogonal to them as well.

2. It remains to establish linear independence. First, note that the $2N$ functions $\phi_{-1,k}^{\text{left}}$ and $\phi_{0,k}^{\text{left}}$, $k = 0, \ldots, N-1$, are all independent. This follows immediately from the staggeredness of their supports: support $\phi_{-1,k}^{\text{left}} = [0, N/2 + k/2]$, support $\phi_{0,k}^{\text{left}} = [0, N + k]$. It follows that the $\tilde{\psi}^k$, $k = 0, \ldots, N-1$, and the $\phi_{0,l}^{\text{left}}$, $l = 0, \ldots, N-1$, also constitute a family of $2N$ independent functions. This is only possible if the $\tilde{\psi}^k$, $k = 0, \ldots, N-1$, are independent. ■

Note that all the $\tilde{\psi}^k$ are supported in $[0, 2N-1]$. Because of the recursion relation (4.7), the $\tilde{\psi}^k$ can be written as a linear combination of $\phi_{-1,l}^{\text{left}}$ and $\phi_{-1,m}$:

$$\tilde{\psi}^k = \sum_{l=0}^{N-1} c_{k,l}\phi_{-1,l}^{\text{left}} + \sum_{m=N}^{3N-2} d_{k,m}\phi_{-1,m}. \tag{4.9}$$

The supports of the $\tilde{\psi}^k$ are not staggered. We can replace the $\tilde{\psi}^k$ by an equivalent family with staggered supports, by essentially the same trick as in Section 3.

PROPOSITION 4.3. *There exists a family of* N *independent functions* $\overset{*}{\tilde{\psi}}{}^k$ *in* W_0^{left}, $k = 0, \ldots, N-1$, *all linear combinations of the* $\tilde{\psi}^k$, *so that* support $\psi^k \subset [0, N+k]$.

Proof.

1. First note that the $\tilde{\psi}^k$ are all orthogonal to $\phi_{0,2N-2} = \sum_{m=-N+1}^{N} h_m \phi_{-1m+4N-4}$. It follows that, for all k,

$$d_{k,3N-3}h_{-N+1} + d_{k,3N-2}h_{-N+2} = 0.$$

2. If $d_{k,3N-2} = 0$ for all k, then choose $\overset{*}{\tilde{\psi}}{}^{N-1} = \tilde{\psi}^{N-1}$, and proceed to the next step. If $d_{k,3N-2} \neq 0$ for some k, reorder the $\tilde{\psi}^k$ so that $d_{N-1,3N-2} \neq 0$, and define $\overset{*}{\tilde{\psi}}{}^{N-1} = \tilde{\psi}^{N-1}$, and, for $k < N-1$, $\tilde{\psi}^{(1),k} = \tilde{\psi}^k - d_{k,3N-2}(d_{N-1,3N-2})^{-1}\tilde{\psi}^{N-1}$. It

follows that the $\tilde{\psi}^{(1),k}$ satisfy a recursion relation similar to (4.9), with the upper limit on the sum over m replaced by $3N-4$. Consequently support $\tilde{\psi}^{(1),k} \subset [0, 2N-2]$ for $k = 0, \ldots, N-2$.

3. We can now repeat these steps, ending up with the desired support property after $N-1$ steps. ▩

The staggered support functions $\tilde{\tilde{\psi}}^k$ satisfy a relation of the same type as (4.9), except that the upper bound on m is now $N+2k$. In a final step, these $\tilde{\tilde{\psi}}^k$ can now be orthonormalized; if we do this by a Gram–Schmidt procedure starting from $k=0$ and working up to larger values of k, the staggered supports are preserved, and we end up with an orthonormal family ψ_k^{left}, $k = 0, \ldots, N-1$. For any $j \in \mathbb{Z}$ we define again $\psi_{-j,k}^{\text{left}}(x) = 2^{j/2}\psi_k^{\text{left}}(2^j x)$. Together with the $\psi_{-j,m}$, $m \geq N$, the $\psi_{-j,k}^{\text{left}}$, $k = 0, \ldots, N-1$, provide an orthonormal basis for W_{-j}^{left}. Moreover, there exists constants $G_{k,l}^{\text{left}}$ and $g_{k,m}^{\text{left}}$ such that

$$\psi_{-j,k}^{\text{left}} = \sum_{l=0}^{N-1} G_{k,l}^{\text{left}} \phi_{-j-1,l}^{\text{left}} + \sum_{m=N}^{N+2k} g_{k,m}^{\text{left}} \phi_{-j-1,m}. \quad (4.10)$$

This completes our explicit construction, at least at a left end. The same of course has to be repeated at a right end.

These right and left end functions can then be used to put together adapted wavelet bases on the interval; following the same indexing conventions as for the scaling functions, we introduce, for $k = 0, \ldots, N-1$

$$\psi^0_{-j,k}(x) = \psi^{\text{left}}_{-j,k}(x) \text{ and } \psi^1_{-j,2^j-k-1}(x) = \psi^{\text{right}}_{-j,-k-1}(x-1).$$

The following theorem then holds.

THEOREM 4.4. *Choose any J so that $2^J \geq 2N$. Then the collection*

$$\bigcup_{j \geq J} [\{\psi^0_{-j,k};\ k = 0, \ldots, N-1\}$$
$$\cup \{\psi_{-j,m};\ m = N, \ldots, 2^j - N - 1\}$$
$$\cup \{\psi^1_{-j,2^j-N+k};\ k = 0, \ldots, N-1\}]$$
$$\cup \{\phi^0_{-J,k};\ k = 0, \ldots, N-1\}$$
$$\cup \{\phi_{-J,m};\ m = N, \ldots, 2^J - N - 1\}$$
$$\cup \{\phi^1_{-J,2^J-N+k};\ k = 0, \ldots, N-1\}$$

is an orthonormal basis for $L^2([0,1])$. If r is the Hölder index of ϕ, ψ (i.e., $\phi, \psi \in C^r$), then this collection is also an unconditional basis for $C^s([0,1])$ for $s < r$; a bounded function f is in $C^s([0,1])$ if and only if

$$|\langle f, \psi^0_{-j,-k}\rangle|,\ |\langle f, \psi_{-j,m}\rangle|,$$
$$|\langle f, \psi^1_{-j,2^j-N+k}\rangle| \leq C 2^{-j(s+1/2)},$$

where C is independent of j and m, k.

Proof. The fact that we have an orthonormal basis follows from the whole construction. The statements about $C^s([0,1])$ (where Zygmund spaces have to be used if s is integer, as always) follow from observations made in Sections 2, 3: the $\psi^0_{-j,k}$, $\psi_{-j,m}$, $\psi^1_{-j,l}$ are all orthogonal to all polynomials of degree $N-1 \geq \lfloor r \rfloor$ (since they are orthogonal to the $\phi^0_{-J,k}$, $\phi_{-J,m}$ and $\phi^1_{-J,l}$ which together generate all polynomials up to degree $N-1$ on $[0,1]$), and, as finite linear combinations of C^r-functions, they are in C^r themselves. ▩

We have therefore achieved our goal: we have a basis with the same good smoothness-characterization potential as Meyer's interval construction, and with moreover the "right" number of scaling functions, and resulting from a numerically stable procedure. As on the whole line, we have no explicit analytic expression for the wavelets and scaling functions on the interval. For practical applications, all that is really needed are the filter coefficients; in addition to the h_m, $g_m = (-1)^m h_{2N+1-m}$, we now also have the $H_{k,l}^{\text{left}}$, $h_{k,m}^{\text{left}}$, $G_{k,l}^{\text{left}}$, $g_{k,m}^{\text{left}}$ (same at right) and their counter-parts. The goal of all the explicit manipulations above was to obtain the constants $H_{k,l}^{\text{left}}$, $h_{k,m}^{\text{left}}$, $G_{k,l}^{\text{left}}$, $g_{k,m}^{\text{left}}$ numerically, so that they could be used in numerical applications. We have carried out all

TABLE 3
The Filter Coefficients $H_{k,l}^{\text{edge}}$, $h_{k,l}^{\text{edge}}$ and $G_{k,l}^{\text{edge}}$ $g_{k,l}^{\text{edge}}$ (as in (4.7), (4.10)) for the Case $N = 2$, for Left and Right Edges

	l	$H_{k,l}$ or $h_{k,l}$	$G_{k,l}$ or $g_{k,l}$
		Left side	
$k = 0$	0	0.6033325119E + 00	−0.7965435169E + 00
	1	0.6908955318E + 00	0.5463927140E + 00
	2	−0.3983129977E + 00	−0.2587922483E + 00
$k = 1$	0	0.3751746045E − 01	0.1003722456E − 01
	1	0.4573276599E + 00	0.1223510431E + 00
	2	0.8500881025E + 00	0.2274281117E + 00
	3	0.2238203570E + 00	−0.8366029212E + 00
	4	−0.1292227434E + 00	0.4830129218E + 00
		Right side	
$k = -2$	−5	0.4431490496E + 00	0.2315575950E + 00
	−4	0.7675566693E + 00	0.4010695194E + 00
	−3	0.3749553316E + 00	−0.7175799994E + 00
	−2	0.1901514184E + 00	−0.3639069596E + 00
	−1	−0.1942334074E + 00	0.3717189665E + 00
$k = -1$	−3	0.2303890438E + 00	−0.5398225007E + 00
	−2	0.4348969980E + 00	0.8014229620E + 00
	−1	0.8705087534E + 00	−0.2575129195E + 00

Note. In every case, the coefficients are listed from left to right ("outermost" coefficients first for the left side, last for the right side). The "interior" h_k are given by $h_{-1} = (1+\sqrt{3})/4\sqrt{2}$, $h_0 = (3+\sqrt{3})/4\sqrt{2}$, $h_1 = (3-\sqrt{3})/4\sqrt{2}$, $h_2 = (1-\sqrt{3})/4\sqrt{2}$ (same as for Table 1).

these computations for the N vanishing moment families with support $[0, 2N-1]$ and closest to linear phase (as constructed in [10]), for $N = 2, 3, \ldots, 10$. We list the coefficients for $N = 2$ and 4, for both left and right edges, in Tables 3 and 4. (The full tables, for other values of N, can be obtained electronically; see the note at the end of the paper.) The corresponding scaling functions and wavelets for both edges are plotted in Figs. 6 and 7. These plots have again been obtained via the cascade algorithm. The adapted wavelets and scaling functions are now less oscillatory than those in Section 3; the overall behavior of their oscillation looks consistent with the behavior of the whole-line functions. It is also quite striking that on $[0, 1]$ the N functions ϕ_k^{left}, $k = 0, \ldots, N-1$, are pure polynomials (of degree $N-1$). This is natural, since all the scaling functions together on $[0, \infty)$ generate the polynomials up to degree $N-1$; since the interior scaling functions $\phi_{0,m}$, $m \geq N$, only start kicking in from $x \geq 1$ onward, the N adapted scaling functions at the left edge cannot be anything but polynomials themselves. (The same is true of course for the right-adapted scaling

TABLE 4

The Filter Coefficients $H_{k,l}^{\text{edge}}$, $h_{k,l}^{\text{edge}}$ and $G_{k,l}^{\text{edge}}$ $g_{k,l}^{\text{edge}}$ (as in (3.2), (3.3)) for the Case $N = 4$, for Left and Right Edges

	l	$H_{k,l}$ or $h_{k,l}$	$G_{k,l}$ or $g_{k,l}$		l	$H_{k,l}$ or $h_{k,l}$	$G_{k,l}$ or $g_{k,l}$
		Left side				Right side	
$k = 0$	0	.90975392E + 00	−.75739704E − 01	$k = -4$	−11	.32210279E − 01	.75771168E − 01
	1	.40416589E + 00	.32543918E + 00		−10	−.12598952E − 01	−.29637661E − 01
	2	.89040317E − 01	−.68434906E + 00		−9	−.99108040E − 01	−.49764705E + 00
	3	−.11984192E − 01	.62004423E + 00		−8	.29771110E + 00	.80379367E + 00
	4	−.30429084E − 01	−.18858513E + 00		−7	.80394959E + 00	−.29778999E + 00
$k = 1$	0	−.27285141E + 00	.16659597E + 00		−6	.49779209E + 00	−.99201918E − 01
	1	.50908154E + 00	−.48478431E + 00		−5	−.30235885E − 01	.12853256E − 01
	2	.62364244E + 00	.35646355E + 00		−4	−.67659162E − 01	.28761869E − 01
	3	.46284008E + 00	.48398963E + 00		−3	−.17709184E − 01	.75281640E − 02
	4	.24674764E + 00	−.60575438E + 00		−2	.19132441E − 01	−.81331898E − 02
	5	−.17669532E − 01	.34518331E − 01		−1	−.67756036E − 02	.28803051E − 02
	6	−.45173645E − 01	.88249013E − 01	$k = -3$	−9	.32148741E − 01	.75756811E − 01
$k = 2$	0	.12611793E + 00	.20825353E + 00		−8	−.12574882E − 01	−.29632043E − 01
	1	−.23085573E + 00	−.40182281E + 00		−7	−.10276635E + 00	−.49684271E + 00
	2	−.52799236E − 01	−.68721488E − 01		−6	.29864734E + 00	.80336362E + 00
	3	.21926518E + 00	.33021352E + 00		−5	.81641197E + 00	−.30158150E + 00
	4	.46348071E + 00	.55802131E + 00		−4	.46061686E + 00	−.95048353E − 01
	5	.70011973E + 00	−.59949744E + 00		−3	.29213680E − 01	.13887372E − 01
	6	.41203257E + 00	−.69091991E − 01		−2	−.13907160E + 00	.30620323E − 01
	7	−.26222762E − 01	.27853571E − 01		−1	.12900783E − 01	.45819595E − 02
	8	−.67040697E − 01	.71209989E − 01	$k = -2$	−7	.41268408E − 01	−.69515191E − 01
$k = 3$	0	−.29079804E − 01	.65485008E − 01		−6	−.16142013E − 01	.27190655E − 01
	1	.59928071E − 01	−.13495243E + 00		−5	−.15813389E + 00	.44993410E + 00
	2	.61764279E − 02	−.13908739E − 01		−4	.39377582E + 00	−.67353457E + 00
	3	−.40211000E − 01	.90551421E − 01		−3	.75400048E + 00	.68118565E − 01
	4	−.39525870E − 01	.89008570E − 01		−2	.44880018E + 00	.50928676E + 00
	5	−.52599061E − 01	.37334445E + 00		−1	−.21916264E + 00	−.27262735E + 00
	6	.32894945E + 00	−.84046537E + 00	$k = -1$	−5	.64379349E − 01	−.99241950E − 01
	7	.79663789E + 00	.31568494E + 00		−4	−.25191808E − 01	.40503097E + 00
	8	.49011302E + 00	.12029765E + 00		−3	.59477713E − 01	−.64952976E + 00
	9	−.29432878E − 01	−.13070202E − 01		−2	.39191428E + 00	.60406780E + 00
	10	−.75247623E − 01	−.33415072E − 01		−1	.91547054E + 00	−.19827799E + 00

Note. In every case, the coefficients are listed from left to right ("outermost" coefficients first for the left side, last for the right side). The "interior" h_k are

$$h_{-3} = .03222310060405, \quad h_{-2} = -.01260396726203, \quad h_{-1} = -.0992195435766,$$
$$h_0 = .29785779560531, \quad h_1 = .8037387518051, \quad h_2 = .4976186676328,$$
$$h_3 = -.02963552764600, \quad h_4 = -.07576571478950.$$

Note that these are in the reverse order from the interior coefficients corresponding to Table 2. In order to get the same ordering as in Table 2, it suffices to exchange "left" and "right" below, and to change the ordering everywhere.

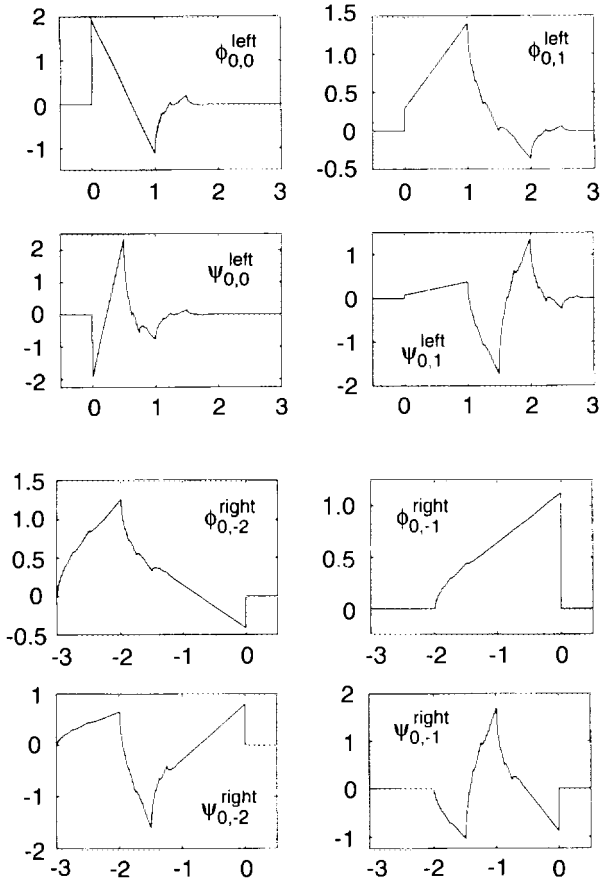

FIG. 6. The two edge scaling functions and wavelets in the case $N = 2$, for left and right sides (i.e., on $[0, \infty)$ or $(-\infty, 0]$). Note that we have two adapted scaling functions at each edge, rather than one, because we have "sacrificed" the first interior function so as to be able to generate all linear polynomials (see text).

functions on $[-1, 0]$.) In the next section we discuss some more properties of and variations on our construction.

5. DISCUSSION OF THE NEW CONSTRUCTION

Many variations are possible on the scheme of Section 4. One can, for instance, start from completely different families of whole-line wavelets. If ϕ has support $[-L + 1, L]$, and $m_0(\xi)$ has a zero of order $K \geq 1$ at $\xi = \pi$, with $K < L$, then there is no need to sacrifice the outermost interior scaling functions $\phi_{-J,L-1}$ and $\phi_{-J,2^J-L-2}$: even if we retain them, we have $2^J - 2L + 2$ interior functions, leaving enough room to add K extra functions at each end, so that all polynomials up to degree $K - 1$ can be generated. If $K < L - 1$, we even have room to spare. If it is important that we have exactly 2^j scaling functions at scale j (as is the case in many applications), then we can add an extra $L - K$ functions almost arbitrarily (without leaving the multiresolution framework, of course—this amounts to adding a few extra sequences of edge filter coefficients); if not, then we can live with just $2^j - 2(L - K)$ scaling functions at each scale j.

The construction in Section 4, and the variation above, assume that we want the scaling functions to generate all possible polynomials up to a certain degree. If the interval wavelets are used to solve a differential equation, then it may be useful to adapt the construction so that all the scaling functions and wavelets involved satisfy certain prescribed boundary conditions. Auscher [2] adapted the original construction by Meyer in this way; his scheme carries over entirely to the present construction (with more numerical stability). The construction by Lemarié-Rieusset, which is essentially the same as ours, obtained independently, was carried out in view of this application.

The same ideas apply of course to biorthogonal wavelet bases. If one starts from a choice with (anti) symmetric wavelets and scaling functions, with filters with an even number of taps (i.e., ϕ, ψ, $\tilde{\phi}$, $\tilde{\psi}$ all have their symmetry axis at $1/2$, with ϕ, $\tilde{\phi}$ symmetric and ψ, $\tilde{\psi}$ antisymmetric), then the adapted scaling functions and wavelets at the right edge can be chosen to be the mirrors of their left edge equivalents. Since orthonormality is not an issue here, but is replaced by biorthogonality, there is more freedom in the choice of the edge functions. One can optimize the adapted edge filters to have, e.g., a total sum of absolute values of their entries as small as possible. If the number of taps in the filters is odd, then it is impossible to have exactly 2^j scaling functions at level j, *and* have adapted scaling functions at the edges that are mirror images of each other. This construction seems therefore less appealing; the obstruction to mirroring is lifted if we allow $2^j + 1$ scaling functions at level j.

Note that in all these constructions we have restricted ourselves to sufficiently fine scales so that the edges do not interact. In the N vanishing moment case with minimal support, this meant that our coarsest scale J was such that $2^J \geq 2N$. What happens if we want to go further? Basically, there is a lot of freedom. If, for instance, N is a power of 2, so that $2^J = 2N$, then at the next stage we have exactly N scaling functions which now touch both edges simultaneously. Since we want them to also generate the N-dimensional space of polynomials up to degree $N - 1$ they all have to be polynomials themselves. How we choose these polynomials determines the filter coefficients at this level; note that this choice is completely unrestricted.

We conclude this paper by pointing out an important difference between wavelets on the line and wavelets on $[0, 1]$, which results in the necessity, in at least some applications, of preconditioning the data (e.g., an image) prior to their wavelet decomposition.

Let us return to the example of the N-vanishing moment family with minimal support. On the whole line, we have

$$\int_{-\infty}^{\infty} dx\, x^l \psi(x) = 0, \quad l = 0, \ldots, N-1,$$

as well as

$$\sum_n n^l g_n = 0, \quad l = 0, \ldots, N-1,$$

or equivalently

$$\sum_n n^l (-1)^n h_n = 0. \tag{5.1}$$

This implies that if we apply our high and low pass filtering to a sequence which is just a linear combination of polynomial sequences, i.e.,

$$c_n = \sum_{l=0}^{N-1} \alpha_l\, n^l, \tag{5.2}$$

the high pass filter yields exactly zero,

$$\sum_n g_{n-2k} c_n = \sum_n (-1)^n h_{2N+1+2k-n} c_n = 0.$$

There is a nice parallelism between the orthogonality of the $\psi(x-n)$ to polynomials and the orthogonality of the high pass filter masks to polynomial sequences. This parallelism can also be expressed otherwise: just as the scaling functions $\phi(x-n)$ generate all polynomials of degree up to $N-1$, the low pass filtering leaves invariant the N-dimensional space of sequences of type (5.2). This is because for any such sequence one can find a polynomial $p(x)$ such that $c_n = \int dx\, p(x)\phi(x-n)$. Consequently $\Sigma_n\, g_{n-2k} c_n = \int dx\, p(x) 2^{-1/2} \psi(x/2 - k) = 0$, and $\Sigma_n\, h_{n-2k} c_n = \int dx\, p(x) 2^{-1/2} \phi(x/2 - k)$, leading to another polynomial sequence. In particular, the sequence $c_n = 1$ can be represented as $c_n = \int dx\, \phi(x-n)$, so that $\Sigma_n\, g_{n-2k} c_n = \int dx 2^{-1/2} \psi(x/2 - k) = 0$.

Things are not that simple on the interval $[0, 1]$. It is still true that the sequence with 2^j entries given by

$$\int dx\, \phi^0_{-j,k}(x), \quad \int dx\, \phi_{-j,m}(x), \quad \int dx\, \phi^1_{-j,2^j-N+l}(x),$$

$$k = 0, \ldots, N-1, m = N, \ldots, 2^j - N - 1, l = 0, \ldots, N-1, \tag{5.3}$$

gets mapped to the zero sequence by the high pass filters adapted to the interval, but the sequence (5.3) is no longer the sequence consisting of only 1's: the edge functions do not have integral 1. The same problem exists in Meyer's construction; the following proposition shows that it is inevitable there.

PROPOSITION 5.1. *Let $\phi^{\text{edge}}_{0,k}$, $k = -N+1, \ldots, N-2$, be the adapted scaling functions constructed as in Section 3 (for, say, a left edge), with $N \geq 2$. Then $\int_0^{2N-2} \phi^{\text{edge}}_{0,k}(x) \neq 1$ for some k. Moreover, if the $\phi^{\#,\text{edge}}_{0,l}$ are the image of the $\phi^{\text{edge}}_{0,k}$ under any $(2N-2) \times (2N-2)$ unitary matrix, then $\int_0^{2N-2} dx \phi^{\#,\text{edge}}_{0,l}(x) \neq 1$ for some l.*

Proof.

1. In Meyer's construction, $\phi^{\text{edge}}_{0,-N+1}$ has support $[0, 1]$, and L^2-norm 1. By Cauchy–Schwarz,

$$\left| \int_0^1 dx\, \phi^{\text{edge}}_{0,-N+1}(x) \right| \leq \|\phi^{\text{edge}}_{0,-N+1}\|^2 = 1,$$

with equality only if $\phi^{\text{edge}}_{0,-N+1}(x) \equiv 1$ on $[0, 1]$. Since this is not the case ($\phi^{\text{edge}}_{0,-N+1}(x) = 0$ for $x > 1$, and the function is continuous), $\int dx \phi^{\text{edge}}_{0,-N+1}(x) \neq 1$.

2. A different orthonormalization of the $\phi^{\text{edge}}_{0,k}$ in Section 3 would lead to $\phi^{\#,\text{edge}}_{0,l}$ related to the $\phi^{\text{edge}}_{0,k}$ by

$$\phi^{\#,\text{edge}}_{0,l} = \sum_{k=-N+1}^{N-2} U_{lk} \phi^{\text{edge}}_{0,k},$$

where U is a $(2N-2) \times (2N-2)$-dimensional unitary matrix. It follows that support $\phi^{\#,\text{edge}}_{0,l} \subset [0, 2N-2]$ for all l, and

$$\int dx\, \phi^{\#,\text{edge}}_{0,l} = \sum_k U_{lk} \int dx\, \phi^{\text{edge}}_{0,k}.$$

If $\int dx\, \phi^{\#,\text{edge}}_{0,l}(x) = 1$ for all l, then this implies that $\Sigma_l |\int dx\, \phi^{\#,\text{edge}}_{0,l}(x)|^2 = 2N - 2$, hence $\Sigma_k |\int_0^{2N-2} dx \phi^{\text{edge}}_{0,k}(x)|^2 = 2N - 2 = |\int_0^{2N-2} dx|^2$. Since the $2N-2$ functions $\phi^{\text{edge}}_{0,k}$ are orthonormal, this is only possible if $\chi_{[0,2N-2]} \in \text{Span}\{\phi^{\text{edge}}_{0,k};\ k = -N+1, \ldots, N-2\}$. But this is again impossible because the $\phi^{\text{edge}}_{0,k}$ are continuous in $2N-2$. ■

In the construction of Section 4 there are only N functions with support $[0, 2N-1]$, so that the same obstruction does not hold. Nevertheless, imposing that at least for one orthonormalization procedure all the scaling functions have integral 1 leads to very stringent requirements on the h_n, which are not satisfied in the "canonical" case of the N vanishing moment family with minimal support. Once one has obtained one orthonormal family of edge scaling functions, it is easy to test whether a possibly different orthonormalization could have led to orthonormal functions with integral 1: this will be the case if and only if $\Sigma_{k=0}^{N-1} |\int dx\, \phi^{\text{left}}_{0,k}(x)|^2 = N$. This last

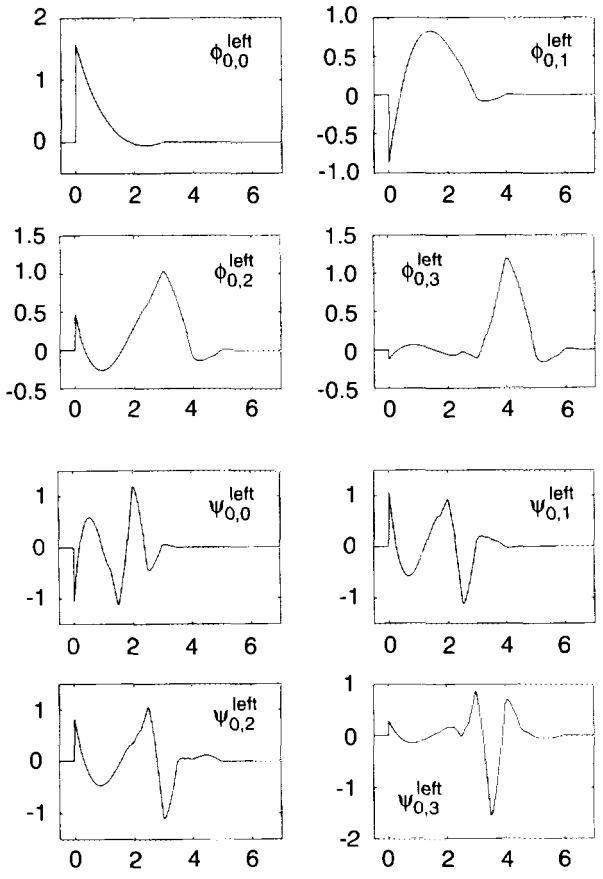

FIG. 7a. The four edge scaling functions and wavelets for the case $N = 4$, for a left edge (i.e., on $[0, \infty)$). Together with the interior scaling functions, the edge scaling functions generate all polynomials of degree 3 or less.

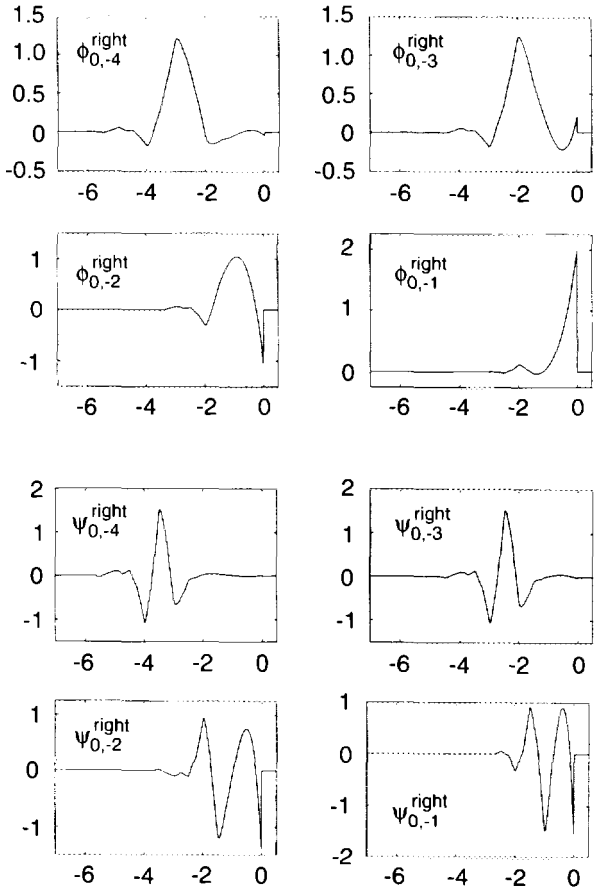

FIG. 7b. Same as in Fig. 7a for a right edge (i.e., on $(-\infty, 0]$).

condition is not verified in the explicit examples computed in Section 4.

In practical examples (e.g., images) one would still like simple polynomial sequences such as 1 1 1 1 $\cdots$ or 1 2 3 4 $\cdots$ to lead to a zero high-pass component, however. This can still be achieved if we perform a prefiltering on the data. The principle is simple. We compute two families of N-dimensional vectors,

$$(V_l)_k = \int dx\, x^l \phi(x - k) \quad k, l = 0, \ldots, N-1,$$
$$(W_l)k = \int_0^\infty dx\, x^l \phi^{\text{left}}_{0,k}(x) \quad k, l = 0, \ldots, N-1. \quad (5.4)$$

The N vectors V_l are trivially independent: if their entries are taken as successive columns of a matrix, the resulting determinant is a nonvanishing Vandermonde determinant. The N vectors W_l are independent as well. If they were not, then there would be a polynomial $p(x)$ of degree $N-1$ orthogonal to all the $\phi^{\text{left}}_{0,k}$, $k = 0, \ldots, N-1$. On the other hand, there exists a finite linear combination of the $\phi^{\text{left}}_{0,k}$ and the $\phi_{0,m}$, $m \geq N$ which coincides with $p(x)$ on $[0, 2N-1]$ and is supported on, say, $[0, 4N]$. Since $p(x)$ is orthogonal to the $\phi^{\text{left}}_{0,-k}$, this linear combination reduces to a linear combination of the $\phi_{0,m}$, $m \geq N$, which implies that it vanishes identically on $[0, 1]$. Since $p \not\equiv 0$ on $[0, 1]$, this is a contradiction.

There exists therefore a (unique) nonsingular $N \times N$-matrix A with nonsingular inverse such that

$$(W_l)_k = \sum_{m=0}^{N-1} A_{km} (V_l)_m.$$

Given a sequence of data, we then apply this matrix to the first N entries,

$$\tilde{c}_k = \sum_{m=0}^{N-1} A_{km} c_m.$$

This maps the polynomial sequences which we would like to map to zero in the high pass filtering to sequences which are polynomial after the first N entries but with specially tailored beginnings. The space of these modified polynomial

sequences is invariant under the low pass filtering operation, and maps to zero under the high pass filters. After this prefiltering operation, the data can be taken through as many high and low pass filtering stages as desired, for a decomposition into wavelets (or wavelet packets, with best basis search). From this decomposed form the data can be reconstructed by the conjugate filtering operations, followed, in the last instance, by a new filtering operation affecting only the N first entries, now using the matrix A^{-1}.

To determine A explicitly, we would have to compute all the quantities in (5.4). This can be done, using the recursion relations as we did above for similar integrals. One can avoid all explicit computations by choosing convenient families of $V_l^\#$, $W_l^\#$ vectors, different from but equivalent to the V_l, W_l. The $V_l^\#$ are defined by

$$(V_l^\#)_k = \binom{k}{l};$$

the correspondence $V_l \leftrightarrow V_l^\#$ is as follows. We know that there is one-to-one correspondence between polynomials of degree $N-1$ and the polynomial coefficient sequences of their expansions in the $\phi(x-n)$. Define the polynomials $q_l(x)$ by

$$q_l(x) = \frac{1}{l!}\sum_{n\in\mathbb{Z}} n(n-1)\cdots(n-l+1)\phi(x-n)$$

$$= \sum_n \binom{n}{l}\phi(x-N+1+n), \quad l=0,\ldots,N-1.$$

Then $(V_l^\#)_k = \int dx\, q_l(x)\phi(x-N+1+k)$. It follows that we should choose $(W_l^\#)_k = \int dx\, q_l(x)\phi^{\text{left}}_{0,N-1-k}(x)$. Note that (4.1) implies that

$$(W_l^\#)_k = \int dx\, \tilde{\phi}^l(x)\phi^{\text{left}}_{0,N-1-k}(x), \tag{5.5}$$

which means that the $(W_l^\#)_k$ are nothing but entries of the orthonormalization matrix giving the transition $\tilde{\phi}^l \to \phi^{\text{left}}_{0,r}$, which we have computed before. It is then easy to obtain A and its inverse. Note that the triangular structure of the arrays $V^\#$, $W^\#$, i.e., $(V_l^\#)_k = 0 = (W_l^\#)_k$ if $l > k$, implies that A and A^{-1} have a similar structure: $A_{km} = 0 = (A^{-1})_{km}$ if $k > m$. All this concerned the left edge only. On the interval, we have to do two prefilterings: one on the leftmost N samples, and another one (with a different matrix) on the rightmost samples. For the N vanishing moment family with minimal support, we have computed these matrices explicitly. For $N = 2$ and 4 the results, for both left and right edge, are listed in Table 5; for other values of N they can be obtained electronically (see the note at the end of the paper).

If one is only interested in the discrete aspect of these filtering operations, as in image subband filtering, then one may well wonder whether this prefiltering is necessary at all. Instead of determining the edge wavelets so that they are orthogonal to polynomials, one can determine the high and low pass filters near the edges so that the high pass filters give zero when applied to polynomial sequences of low degree. This is the point of view adopted by Herley and Vetterli [14]; it avoids the need of preconditioning. The same phenomenon is, however, still present, in a disguised form: even though $1\,1\,1\,1\,1\cdots$ and $1\,2\,3\,4\,5\cdots$ map to zero under the high pass filters, the space of polynomial sequences is not preserved under the low pass filters. At the next stage, their low pass versions are transformed into adulterated polynomial sequences, and these do not map to zero under the high pass filtering operation. Our prefiltering introduces an extra step, but after this (non unitary) step, everything is stable in the sense that an originally polynomial sequence leads to zero content in all the band pass channels afterwards. If one works with biorthogonal instead of orthonormal wavelets, then there is so much more freedom in the choice of the edge functions that it is possible to construct biorthogonal schemes in which the low pass filters automatically preserve polynomial sequences, so that no prefiltering is necessary.

APPENDIX A: PROOF OF AN IDENTITY USED IN SECTION 2

PROPOSITION A.1. *Let ψ, $\tilde{\psi}$ be dual functions generating biorthogonal wavelet bases as in Cohen et al.* [8]. *If $\int dx\, H(x)\tilde{\psi}(x-m) = 0$ for all $m \in \mathbb{Z}$, where $H(x) = 1 - |x|$ for $|x| \le 1$, $H(x) = 0$ otherwise, then $\phi(x) = H(x-L)$ for some $L \in \mathbb{Z}$.*

Proof. We use the notations of Cohen *et al.* [8] throughout this proof.

1. Using the recursion $\tilde{\psi}(x) = \sqrt{2}\ \Sigma_k\ (-1)^k\overline{h_{-k+1}}\,\tilde{\phi}(2x-k)$, we find that $\Sigma_k\,(-1)^k\overline{h_{-k+1}}\alpha_{2m-k} = 0$ for all $m \in \mathbb{Z}$, where $\alpha_m = \int dx\, H(x)\tilde{\phi}(2x+m)$. With the notation $\alpha(\xi) = \Sigma_m\, \alpha_m e^{-im\xi}$, this can be rewritten as

$$\overline{m_0(\xi+\pi)}\,\alpha(\xi) - \overline{m_0(\xi)}\,\alpha(\xi+\pi) = 0.$$

Since $m_0(\xi)$, $m_0(\xi+\pi)$ do not vanish together, this implies that

$$\alpha(\xi) = \overline{m_0(\xi)}\,\nu(2\xi); \tag{A.1}$$

because only finitely many α_k are non-zero ($\tilde{\phi}$ has compact support), both α and ν are trigonometric polynomials.

2. Because $\overline{m_0(\xi)}\tilde{m}_0(\xi) + \overline{m_0(\xi+\pi)}\tilde{m}_0(\xi+\pi) = 1$, we conclude from (A.1) that

$$\nu(2\xi) = \tilde{m}_0(\xi)\alpha(\xi) + \tilde{m}_0(\xi+\pi)\alpha(\xi+\pi),$$

TABLE 5

The Preconditioning Matrices Corresponding to the Edge Filters of Tables 3 and 4

$N = 2$

$$A_{\text{left}} = \begin{pmatrix} 0.32540489\text{E}+00 & 0.00000000\text{E}+00 \\ 0.37158015\text{E}-01 & 0.10014454\text{E}+01 \end{pmatrix},$$

$$A_{\text{left}}^{-1} = \begin{pmatrix} 0.30779265\text{E}+01 & 0.00000000\text{E}+00 \\ -0.11420457\text{E}+00 & 0.99855668\text{E}+00 \end{pmatrix}$$

$$A_{\text{right}} = \begin{pmatrix} 0.10898431\text{E}+01 & -0.80081323\text{E}+00 \\ 0.00000000\text{E}+00 & 0.20962929\text{E}+01 \end{pmatrix},$$

$$A_{\text{right}}^{-1} = \begin{pmatrix} 0.91756331\text{E}+00 & 0.35052203\text{E}+00 \\ 0.00000000\text{E}+00 & 0.47703258\text{E}+00 \end{pmatrix}$$

$N = 4$

$$A_{\text{left}} = \begin{pmatrix} 0.24899111\text{E}+01 & 0.00000000\text{E}+00 & 0.00000000\text{E}+00 & 0.00000000\text{E}+00 \\ -0.27529885\text{E}+01 & 0.16772106\text{E}+01 & 0.00000000\text{E}+00 & 0.00000000\text{E}+00 \\ 0.16878414\text{E}+01 & -0.70753754\text{E}+00 & 0.11301451\text{E}+01 & 0.00000000\text{E}+00 \\ -0.40222212\text{E}+00 & 0.17635443\text{E}+00 & -0.61621216\text{E}-01 & 0.10068852\text{E}+01 \end{pmatrix}$$

$$A_{\text{left}}^{-1} = \begin{pmatrix} 0.4016208\text{E}+00 & 0.00000000\text{E}+00 & 0.00000000\text{E}+00 & 0.00000000\text{E}+00 \\ 0.65922394\text{E}+00 & 0.59622806\text{E}+00 & 0.00000000\text{E}+00 & 0.00000000\text{E}+00 \\ -0.18709675\text{E}+00 & 0.37327395\text{E}+00 & 0.88484210\text{E}+00 & 0.00000000\text{E}+00 \\ 0.33523746\text{E}-01 & -0.81584146\text{E}-01 & 0.54152199\text{E}-01 & 0.99316192\text{E}+00 \end{pmatrix}$$

$$A_{\text{right}} = \begin{pmatrix} 0.10003981\text{E}+01 & -0.22411543\text{E}-02 & -0.18445047\text{E}-01 & -0.73733049\text{E}-02 \\ 0.00000000\text{E}+00 & 0.10023130\text{E}+01 & 0.91704628\text{E}-01 & -0.93100685\text{E}-03 \\ 0.00000000\text{E}+00 & 0.00000000\text{E}+00 & 0.78081762\text{E}+00 & 0.37673864\text{E}+00 \\ 0.00000000\text{E}+00 & 0.00000000\text{E}+00 & 0.00000000\text{E}+00 & 0.00000000\text{E}+00 \end{pmatrix}$$

$$A_{\text{right}}^{-1} = \begin{pmatrix} 0.99960208\text{E}+00 & 0.22350928\text{E}-02 & 0.23350830\text{E}-01 & -0.28464600\text{E}-02 \\ 0.00000000\text{E}+00 & 0.99769238\text{E}+00 & -0.11717590\text{E}+00 & 0.90053579\text{E}-01 \\ 0.00000000\text{E}+00 & 0.00000000\text{E}+00 & 0.12807088\text{E}+01 & -0.96398392\text{E}+00 \\ 0.00000000\text{E}+00 & 0.00000000\text{E}+00 & 0.00000000\text{E}+00 & 0.19979252\text{E}+01 \end{pmatrix}$$

Note. For each of the cases $N = 2$, $N = 4$, we list A and its inverse A^{-1}, first for the left side, then for the right side. They should be applied as follows: arrange all the data points in one column vector d, with entries $d_1 \cdots d_L$ ($L \geq 2N$). Apply A_{left} to the N-vector with entries $d_1 \cdots d_N$, A_{right} to the N-vector with entries $d_{L-N+1} \cdots d_L$ (in that order), and use the results to replace $d_1 \cdots d_N$ and $d_{L-N+1} \cdots d_L$; the $d_{N+1} \cdots d_{L-N}$ are not touched. The resulting sequence is the preconditioned sequence. After decomposition + reconstruction by means of interior and edge filters, the same procedure should be followed (with A_{left}^{-1} and A_{right}^{-1}) to recover the original data.

or, equivalently, $\nu(\xi) = \Sigma_k \nu_k e^{-ik\xi}$ with

$$\nu_k = \sqrt{2} \sum_l \tilde{h}_l \alpha_{2k-l} = \sqrt{2} \sum_l \tilde{h}_l \int dx\, H(x) \tilde{\phi}(2x + 2k - l)$$

$$= \int dx\, H(x) \tilde{\phi}(x + k).$$

3. On the other hand, $H(x) = \frac{1}{2} H(2x + 1) + H(2x) + \frac{1}{2} H(2x - 1)$, which leads to

$$\alpha_k = \tfrac{1}{4}\nu_{k-1} + \tfrac{1}{2}\nu_k + \tfrac{1}{4}\nu_{k+1}.$$

This implies that $\alpha(\xi) = (\cos^2 \xi/2)\nu(\xi)$; hence

$$\left(\cos^2 \frac{\xi}{2}\right)\nu(\xi) = \overline{m_0(\xi)}\, \nu(2\xi).$$

4. Because $\int dx\, x\tilde{\psi}(x) = 0$, $m_0(\xi)$ is divisible by $\cos^2 \xi/2$, so that

$$\nu(\xi) = \nu(2\xi) Q(\xi),$$

where Q is a trigonometric polynomial. Consequently if $z_0 = e^{i\xi_0}$ corresponds to a zero of ν (where $|z_0|$ may be $\neq 1$), then so does $z_0/2$. Since there can only be finitely many such zeros, this implies that $\nu(\xi) = Ce^{-iL\xi}$ for some $L \in \mathbb{Z}$.

5. It follows that $\alpha(\xi) = C \cos^2(\xi/2) e^{-iL\xi}$; substituting this into (A.1) gives

$$\overline{m_0(\xi)} = C \cos^2 \frac{\xi}{2} e^{-iL\xi} e^{2iL\xi},$$

or $m_0(\xi) = C \cos^2(\xi/2) e^{-iL\xi}$, leading to $C = 1$ and $\phi(x) = H(x - L)$. ■

NOTE ON ELECTRONIC AVAILABILITY OF MORE COMPLETE TABLES

Complete tables for $N = 2$ to 8, for Meyer's construction as well as the new construction, are available by ftp; node: research.att.com; user name: netlib, password: your e-mail address; directory: stat/data. The file is in binary and is called wavelets.Z. You should uncompress it after acquiring it. You can also get the file by sending the message

send /stat/data/wavelets

to netlib@research.att.com. The part of the tables concerning only the new construction is also available from an ftp node in Europe; node: ftp.ensta.fr, user name: anonymous, password: your e-mail address, directory: pub, filename: tables; this file is in ASCII. The tables in these files, like those in this paper, are accurate to 10^{-8}. For most purposes this is amply sufficient; more accurate tables (to 10^{-14}) have been computed by Mary Brewster and Greg Beylkin.

ACKNOWLEDGMENTS

A. Cohen and P. Vial thank the Mathematics Center of AT&T Bell Laboratories, where this work was carried out, for hospitality and support. We also thank the referees for reading the manuscript very carefully and finding many small mistakes. We are grateful to Minh Do Kac for pointing out a wrong figure and to Mary Brewster and Greg Beylkin for drawing our attention to wrong entries in the tables.

Note Added in Proof. It has come to our attention that there exists yet another approach to the construction of wavelet bases on the interval, without wrap-around effects, with 2^j wavelets and 2^j scaling functions at scale j, in M. H. Freedman and W. H. Press, "Truncation of Wavelet Matrices: Edge Effects and the Reduction of Topological Control," University of California, San Diego, preprint (December 1992).

REFERENCES

1. L. Andersson, N. Hall, B. Jawerth, and G. Peters, Wavelets on closed subsets of the real line, *in* "Topics in the Theory and Applications of Wavelets" (Larry L. Schumaker and Glenn Webb, Eds.), Academic Press, Boston, to appear.
2. P. Auscher, Ondelettes à support compact et conditions aux limites, to appear in *J. Funct. Anal.* **111** (1993), 29–43.
3. M. Berger, Random affine iterated function systems: Curve generation and wavelets, *SIAM Rev.* **34** (1992), 361–385.
4. A. Cohen and I. Daubechies, A stability criterion for biorthogonal wavelet bases and their related subband coding scheme, *Duke Math. J.* **68** (1992), 313–335.
5. A. Cohen, I. Daubechies, B. Jawerth, and P. Vial, Multiresolution analysis, wavelets and fast algorithms on an interval, *C. R. Acad. Sci. Paris Ser. I Math.* **316** (1992), 417–421.
6. A. S. Cavaretta, W. Dahmen, and C. Micchelli, Stationary subdivision, *Mem. Amer. Math. Soc.* **93** (1991), 1–186.
7. A. Cohen, Ondolettes, analyses multirésolutions et filtres miroir en quadrature, *Ann. Inst. H. Poincaré Anal. Non Linéaire* **7** (1990), 439–459.
8. A. Cohen, I. Daubechies, and J. C. Feauveau, Biorthogonal bases of compactly supported wavelets, *Comm. Pure Appl. Math.* **45** (1992), 485–560.
9. I. Daubechies, Orthonormal bases of compactly supported wavelets, *Comm. Pure Appl. Math.* **41** (1988), 909–996.
10. I. Daubechies, "Ten Lectures on Wavelets," CBMS Lecture Notes, No. 61, SIAM, Philadelphia, 1992.
11. I. Daubechies, Orthonormal bases of compactly supported wavelets. II. Variations on a theme, *SIAM J. Math. Anal.* **24** (1993), 499–519.
12. I. Daubechies and J. Lagarias, Two-scale difference equations. I. Existence and global regularity of solutions, *SIAM J. Math. Anal.* **22** (1991), 1388–1410; Two-scale difference equations. II. Local regularity, infinite products of matrices and fractals, *SIAM J. Math. Anal.* **23** (1992), 1031–1079.
13. G. Fix and G. Strang, Fourier analysis of the finite element method in Ritz–Galerkin theory, *Stud. Appl. Math.* **48** (1969), 265–273.
14. C. Herley and M. Vetterli, Time-varying orthogonal filterbanks and wavelets, submitted for publication a shorter discussion is in C. Herley, J. Kovačević, K. Ramchandran, and M. Vetterli, Time-varying orthonormal tilings of the time-frequency plane, *IEEE Trans. Signal Process.*, to appear.
15. P. G. Lemarié and G. Malgouyres, Support des fonctions de base dans une analyse multirésolution, *C. R. Acad. Sci. Paris* **313** (1991), 377–380.
16. A. Jouini and P. G. Lemarié-Rieusset, Analyses multirésolutions biorthogonales et applications, *Ann. Inst. H. Poincaré Anal. Non Linéaire*, to appear.
17. W. Lawton, Tight frames of compactly supported wavelets, *J. Math. Phys.* **31** (1990), 1898–1901.
18. W. Lawton, Necessary and sufficient conditions for constructing orthonormal wavelet bases, *J. Math. Phys.* **32** (1991), 57–61.
19. S. Mallat, Multiresolution approximation and wavelets, *Trans. Amer. Math. Soc.* **315** (1989), 69–88.
20. Y. Meyer, "Ondelettes et opérateurs. I. Ondelettes. II. Opérateurs de Calderón–Zygmund. III. Opérateurs multilinéaires," Hermann, Paris, 1990, English translation, Cambridge Univ. Press, London/New York, 1993.
21. Y. Meyer, Ondelettes due l'intervalle, *Rev. Mat. Iberoamericana* **7** (1992), 115–133.